Renewable and Sustainable Energy Reviews 31 (2014) 870–906

Contents lists available at ScienceDirect

Renewable and Sustainable Energy Reviews

journal homepage: www.elsevier.com/locate/rser

Phase change materials integrated in building walls: A state of the art review

Shazim Ali Memon *

Department of Civil and Architectural Engineering, City University of Hong Kong, Hong Kong

ARTICLE INFO

Article history:
Received 23 August 2013
Received in revised form
4 November 2013
Accepted 20 December 2013
Available online 24 January 2014

Keywords:
Thermal energy storage
Phase change materials
Building applications
Form-stable composite PCM

ABSTRACT

The building sector is the dominant energy consumer with a total 30% share of the overall energy consumption and accounts for one-third of the greenhouse gas emissions around the world. Moreover, in recent years the energy demands for buildings have increased very rapidly due to increase in the growth rate of population and improvement in living standards of people. Furthermore, fossil fuels will continue to dominate the world's primary energy by 2030. Thus, the increase in energy demand, shortage of fossil fuels and environmental concerns has provided impetus to the development of sustainable building and renewable energy resources. Thermal energy storage is an efficient method for applying to building envelopes to improve the energy efficiency of buildings. This, in turn, reduces the environmental impact related to energy usage.

The combination of construction materials and PCM is an efficient way to increase the thermal energy storage capacity of construction elements. Therefore, an extensive review on the incorporation of PCM into construction materials and elements by direct incorporation, immersion, encapsulation, shape-stabilization and form-stable composite PCMs is presented. For the first time, the differentiation between shape-stabilized and form-stable composite PCM has been made. Moreover, various construction materials such as diatomite, expanded perlite and graphite, etc. which are used as supports for form-stable composite PCM along with their worldwide availability are extensively discussed. One of the main aims of this review paper is to focus on the test methods which are used to determine the chemical compatibility, thermal properties, thermal stability and thermal conductivity of the PCM. Hence, the details related to calibration, sample preparation, test cell and analysis of test results are comprehensively covered. Finally, because of the renewed interest in integration of PCM in wallboards and concrete, an up-to-date review with focus on PCM enhanced wallboard and concrete for building applications is added.

Contents

* Tel.: +852 27888782.
E-mail address: shazimalimemon@gmail.com

1364-0321/$ - see front matter © 2014 Elsevier Ltd. All rights reserved.
http://dx.doi.org/10.1016/j.rser.2013.12.042

1. Introduction

The rapid economic growth worldwide has lead to increase in the energy demand. According to the International Energy Agency (IEA) statistics (Fig. 1) [1], fossil fuel are dominating the world energy market with a share of around 81% and it is predicted that it will continue to dominate the world's primary energy by 2030 [2]. However, the conventional fossil energy sources are depleting, and their usage is related to the emission of harmful gases making people worried about environmental issues and a shortage of energy resources. To deal with this demanding situation, energy resources should be used proficiently.

The building sector is the dominant energy consumers around the world with a total of 30% share of the overall energy consumption [3]. This share is on the higher side in developed countries, for example in U.S., it accounts for 41% share of primary energy (Fig. 2) [4]. Moreover, in recent years the energy demands for buildings have increased very rapidly due to increase in the growth rate of population and improvement in living standards of people [5]. Thus, improving the energy consumption of buildings would not only reduce the dependence on fossil fuel but would also have a major impact on the total greenhouse gas emissions. Thermal energy storage is an efficient method for applying to building envelopes to improve the energy efficiency of buildings. This, in turn, would reduce the environmental impact related to energy usage [6].

In this review, firstly the desirable properties governing the selection of PCM are presented. Section 3 covers the classification of PCMs, their merits and demerits and includes the list of PCM that are suitable for building applications. The incorporation of PCM into construction materials and elements by direct incorporation, immersion, encapsulation, shape-stabilization and form-stable composite PCMs is discussed in Section 4. Moreover, various porous construction materials such as diatomite, expanded perlite, expanded graphite, etc used as supports for form-stable composite PCM along with their worldwide availability are extensively discussed in this section. Sections 5–8 extensively discuss the test

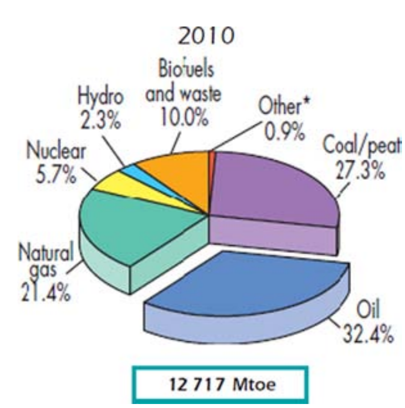


Fig. 1. World total primary energy supply by fuel in 2010 [1].

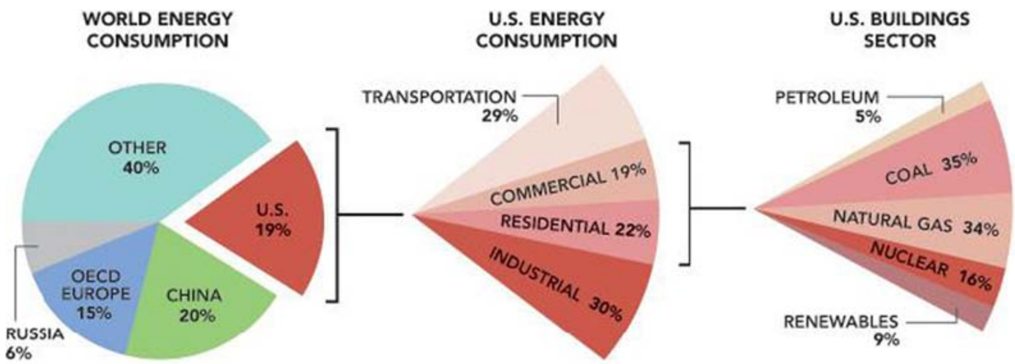


Fig. 2. Energy consumed by building sector in U.S [4].

Table 1
Desirable properties governing the selection of PCM.

Thermal-physical properties
- Phase change temperature suitable for building application
- High latent heat of fusion per unit volume so that smaller size of container can be used
- High thermal conductivity to assist in charging and discharging of PCM within the limited time frame
- High specific heat so that additional energy in the form of sensible heat is available to the thermal energy storage system
- Small volume change during phase transition and small vapour pressure at operating temperature so as to avoid the containment problem
- PCM should melt completely (i.e. congruent melting) during phase transition so that the solid and liquid phases are homogenous
- Thermally reliable (i.e. cycling stability) so that PCM is stable in terms of phase change temperature and latent heat of fusion and can be used in long run

Kinetic properties
- High rate of nucleation so as to avoid supercooling of the PCM in liquid phase
- High rate of crystal growth so that heat recovery from the storage system is optimum

Chemical properties
- Chemically compatible with construction/encapsulated materials
- No degradation after large number of thermal (freeze/melt) cycles so as to assure long operation life
- Non-toxic, non-flammable and non-explosive so as to assure safety
- Corrosion resistant to construction/encapsulated materials

Economic properties
- Cost effective
- Commercially available

Environmental properties
- Low environmental impact and non-polluting during service life
- Having recycling potential

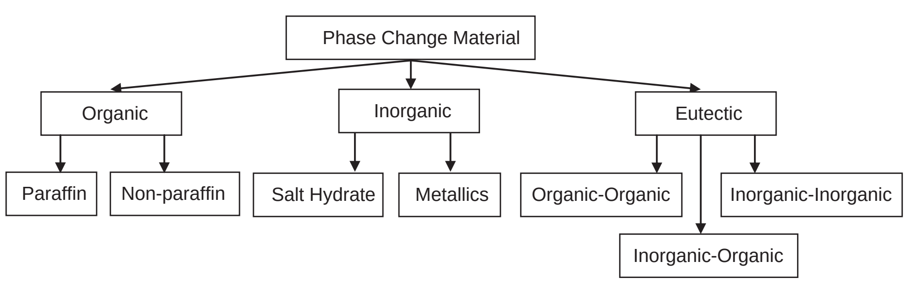


Fig. 3. Classification of PCMs [7].

methods which are used to determine the chemical compatibility, thermal properties, thermal stability and thermal conductivity of the PCM. For some of the main test methods, the details related to calibration, sample preparation, test cell and analysis of test results are also covered. Section 9 is on the thermal conductivity enhancement of PCM. Finally, a separate section with focus on PCM enhanced wallboard and concrete for building applications is added.

2. Desirable properties governing the selection of PCM

In order to be used for building applications, the PCM must possess certain desirable thermal-physical, kinetic, chemical, economic and environmental properties (Table 1) [6–12]. It is worth mentioning here that no PCM can have all the desirable properties. Therefore, the choice of a PCM for a given thermal energy storage application in buildings require careful examination of the thermo-physical, kinetic, chemical, economic and environmental properties of the various available candidates, comparing their merits and demerits and in some cases achieving a certain degree of compromise [13].

3. Classification of PCMs

In 1983, Abhat [14] introduced a valuable classification of PCMs for thermal energy storage applications. Based on the chemical composition, PCM can be classified as organic, inorganic and

ectectic (Fig. 3). The merits and demerits of different types of PCMs are summarized in Table 2 [10,12,15–19].

Some of organic, inorganic and eutectic PCM suitable for building applications and in the temperature range of 18 °C to 40 °C are listed in Tables 3–5. The upper temperature limit is justified by the fact that the surface temperatures of roofs and external walls of building can reach 40 °C and above [20].

Table 2
Merits and de-merits of PCMs.

Organic PCM – Paraffin and non-paraffin

Advantages

- Available in large temperature range (from approximately 20 °C up to about 70 °C)
- Chemically inert
- Do not undergo phase segregation
- Thermally reliable in long run (freeze melt cycle)
- Have low vapour pressure in the melt form
- Reasonable latent heat of fusion (120 J/g up to 210 J/g)
- Paraffins have high specific heat than salt hydrates
- Non-corrosive, however, fatty acids are mildly corrosive
- Inexpensive, however, fatty acids are 2–2.5 times expensive than technical grade paraffin
- Compatible with construction materials
- Small volume change during phase transition
- Little or no supercooling during freezing
- Innocuous (Neither toxic nor irritant, however, non-paraffins show varying level of toxicity)
- Stable below 500 °C, however, non-paraffins show instability at high temperature
- Recyclable

Disadvantages

- Low thermal conductivity (around 0.2 W/m.K)
- Moderately flammable
- Non-compatible with plastic containers

Inorganic PCM – Salt hydrates

Advantages

- High volumetric latent heat storage (Almost double than that of organic materials)
- High latent heat of fusion
- High thermal conductivity (0.5 W/m.K)
- Cheaper and readily available
- Non-flammable
- Compatible with plastic containers
- Sharp phase change
- Low environmental impact
- Having recycling potential

Disadvantages

- Undergo supercooling during freezing
- Undergo phase segregation during transition
- Corrosive to most metals
- Irritant
- Have high vapor pressure (Induce water loss and cause progressive change in thermal behavior during thermal cycling process)
- May show long term degradation by oxidization, hydrolysis, thermal decomposition and other reactions
- Exhibit variable chemical stability
- High volume change

Eutectic

Advantages

- In general have sharp melting temperature
- High volumetric thermal storage density (slightly above organic PCM)

Disadvantages

- Limited test data available on their thermo-physical properties

4. Incorporation of PCM into construction materials and elements

The PCM can be incorporated in construction materials and elements by direct incorporation, immersion, encapsulation, shape-stabilization and form stable composite PCMs.

4.1. Direct incorporation

This is the simplest, practicable and economical method in which PCM is directly mixed with the construction materials for example gypsum, cement paste, mortar or concrete during production [32,33]. For successful utilization of PCM especially into cement based materials it should not (a) interface with the hydration process and hydration products [32] (b) affect the bonding between the paste and the aggregate [32] (c) affect the mechanical properties and (d) affect the durability properties. However, leakage of the PCM may interfere with the hydration products and may affect the mechanical and durability properties of the system.

4.2. Immersion

In the immersion technique, the construction elements (concrete and brick blocks, wall boards), which are dipped into the liquid PCM, absorb the PCM by capillary action [32]. It is reported that PCM may leak [10,11,16] especially after subjected to large number of thermal cycles. Also, it may affect the mechanical and durability properties of the construction elements.

It is worth mentioning here that both direct and immersion techniques incorporate PCM directly into the conventional construction materials.

4.3. Encapsulation

In this technique, PCM has to be encapsulated before being used into construction elements. It has been pointed out by Regin et al. [8] that PCM encapsulation should (a) meet the requirement of strength, durability and thermal stability and reliability (b) protect the PCM, by acting as a barrier, from destructive interactions with the surrounding environment (c) have sufficient surface area for efficient heat transfer (d) be structurally stable and provide ease in handling. In general, two PCM encapsulation methods are reported – microencapsulation and macroencapsulation [9–11,17].

4.3.1. Microencapsulation

In microencapsulation, small PCM particles ranging from 1 μm to 1000 μm are enclosed in a thin solid shell usually made from natural and synthetic polymers [9,34]. The phase change materials having phase change temperatures in between −10 and 80 °C can be manufactured with this technique [35]. Two methods (physical and chemical) of microencapsulation have been reported in the literature [35]. The physical methods include pan coating, air-suspension coating, centrifugal extrusion, vibrational nozzle and spray drying while the chemical methods include coacervation, complex coacervation and interfacial methods [35]. Microencapsulation has the following advantages [10,17,34,36].

(a) Prevents the leakage of PCM during phase transition by building a barrier thereby increasing its chances of incorporation into various construction materials.
(b) Provide high heat transfer rate through its larger surface area per unit volume.
(c) Capable of resisting volume change during phase transition.
(d) Improved chemical stability as demonstrated by Alkan et al. and Ozonu et al. [37,38].
(e) Improved thermal reliability as demonstrated Hawlader et al., Alkan et al. and Ozonu et al. [37–39] and since phase

separation during transition is limited to microscopic distances.

Some issues also exist in microencapsulation as pointed out by various researchers.

(a) The rigidity of the shell prevents natural convection and therefore decreases the heat transfer rate [8].
(b) Microencapsulation may affect the mechanical properties of the construction materials [22]. However, Cabeza et al. [40] showed that microencapsulated concrete (Mopcon concrete) satisfied the requirement for general structural purpose [11].
(c) High investment cost renders its feasibility to reach commercial state.

Some of the prominent studies mainly focusing on the preparation and characterization of microencapsulated PCMs are discussed herein.

Alkan et al. [37] developed microencapsulated PCM through emulsion polymerization with *n*-docosane as phase change material and polymethylmethacrylate as shell material for thermal energy storage applications. SEM micrographs (Fig. 4) showed that the microcapsules have smooth and compact surfaces and have spherical profiles. The average size of the microcapsules determined by particle size distribution was found to be 0.16 mm. FT-IR results showed that docosane and polymethylmethacrylate are chemically compatible. From DSC analysis, the melting and crystallization temperatures of docosane in microcapsules were found to be 41.0 °C and 40.6 °C while the latent heat of melting and crystallization were found to be 54.6 and 48.7 J/g respectively. Thus, microcapsules successfully contained 28 wt% of docosane. Thermal cycling test showed that the changes observed in the thermal properties and chemical structure of microcapsulated PCM after 5000 melting/freezing cycles are very little and in the acceptable range. Based on the test results, it was concluded that the composite PCM has considerable potential for thermal energy storage applications.

Hawlader et al. [39] assessed the performance of microencapsulated PCM for thermal energy storage applications through

Table 3
Organic PCM – Paraffin and non-paraffin.

PCM	Melting temperature (°C)	Heat of fusion (J/kg K)	References
Propyl palmitate	16–19	186	[17,21,22]
Glycerin	17.9	198.7	[7]
Hexadecane	18.1	236	[15,23]
Butyl stearate	19	140	[11,18,21,24]
Propyl palmitate	19	186	[11,21,24]
Paraffin C_{16}–C_{18}	20–22	152	[17,18,21,24]
Heptadecane	20.8–21.7	171–172	[25]
Dimethyl sabacate	21	120–135	[11,18,21,24]
Octadecyl 3-mencaptopropylate	21	143	[11,21]
Paraffin C_{17}	21.7	213	[7,17]
Polyglycol E600	22	127.2	[17,18,21,24]
Paraffin C_{13}–C_{24}	22–24	189	[17,18,21,24]
Octadecyl thioglyate	26	90	[17,21]
Lactic acid	26	184	[7,17]
1-Dodecanol	26	200	[17,18,24]
Vinyl stearate	27–29	122	[17,18,21,24]
Octadecane	28–28.1	244–250.7	[15]
Paraffin C_{18}	28	244	[7,17,18,21,24]
Methyl palmitate	29	205	[7]
Capric acid	30.1	158	[15,26–28]
Camphenilone	39	205	[7]
Docasyl bromide	40	201	[7]
Caprylone	40	259	[7]

Table 4
Inorganic PCM – Salt hydrates.

PCM	Melting temperature (°C)	Heat of fusion (J/kg K)	References
$KF \cdot 4H_2O$	18.5	231	[14,18,29]
$FeBr_3 \cdot 6H_2O$	21	105	[7,17]
$Mn(NO_3)_2 \cdot 6H_2O$	25.8	125.9	[18,30]
$CaCl_2 \cdot 6H_2O$	29–30	171–192	[13,18]
$CaCl_2 \cdot 12H_2O$	29.8	174	[7,17]
$LiNO_3 \cdot 3H_2O$	30	296	[18]
$Na_2SO_4 \cdot 10H_2O$	31–32.4	251.1–254	[14,18,29,31]
$Na_2SO_4 \cdot 3H_2O$	32	251	[17,21]
$Na_2CO_3 \cdot 10H_2O$	32–36	246.5–247	[18,31]
$CaBr_2 \cdot 6H_2O$	34	115.5	[13,18,31]
$LiBr_2 \cdot 2H_2O$	34	124	[7,17]
$Na_2HPO_4 \cdot 12H_2O$	35–36	265–281	[29,31]
$Zn(NO_3)_2 \cdot 6H_2O$	36–36.4	146.9–147	[13,14,29,31]
$FeCl_3 \cdot 6H_2O$	37	223	[17,18]

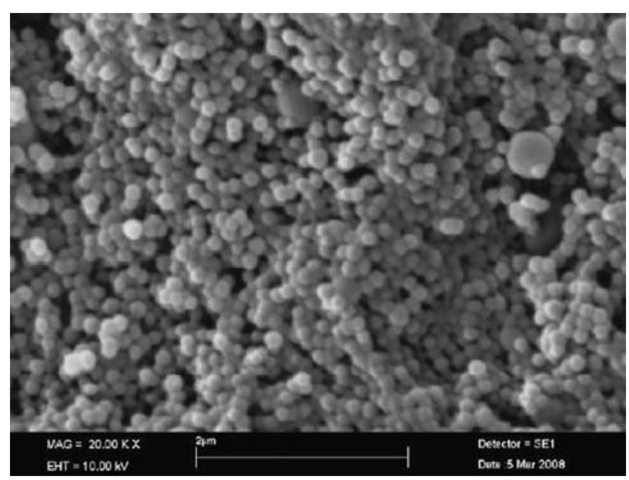


Fig. 4. SEM image of Polymethylmethacrylate/docosane microcapsules [37].

Table 5
Eutectic PCM – Organic and inorganic.

PCM	Melting temperature (°C)	Heat of fusion (J/kg K)	References
$34\%C_{14}H_{28}O_2 + 66\% C_{10}H_{20}O_2$	24	147.7	[7,17]
$50\%CaCl_2 + 50\%MgCl_2 \cdot 6H_2O$	25	95	[7]
Octadecane + docosane	25.5–27	203.8	[15,17]
Octadecane + heneicosane	25.8–26	173.93	[15,17]
$50\%CH_3CONH_2 + 50\% NH_2CONH_2$	27	163	[7,17]
Ga	30	80.9	[7,17]
$47\%Ca(NO_3)_2 \cdot 4H_2O + 53\%Mg(NO_3)_2 \cdot 6H_2O$	30	136	[17,18,24]
$60\%Na(CH_3COO) \cdot 3H_2O + 40\%CO(NH_2)_2$	30–31.5	200.5–226	[7,17,18,21,24]

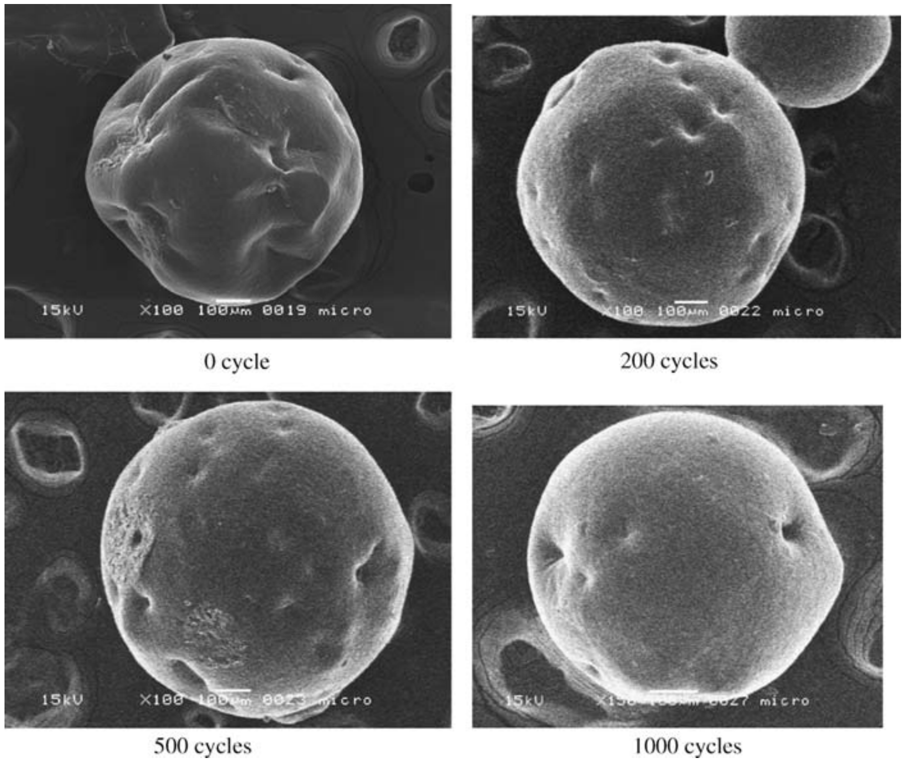


Fig. 5. Microencapsulated paraffin profile evaluated by SEM at different thermal cycles [39].

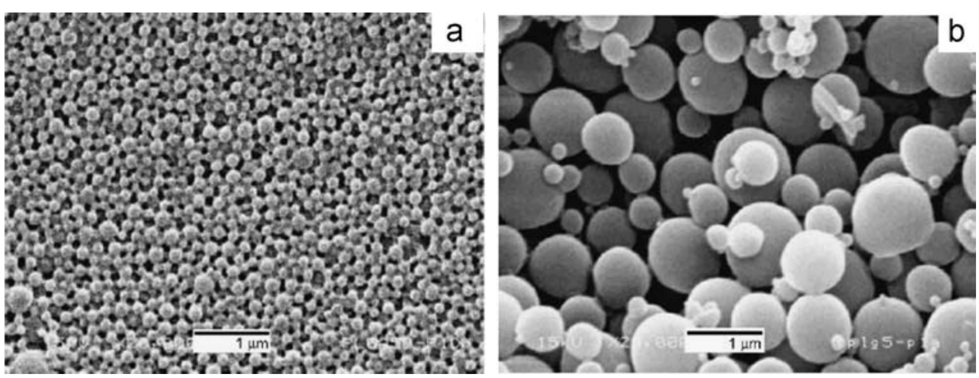


Fig. 6. SEM profile for (a) spray-dried (b) concervated microparticles [34].

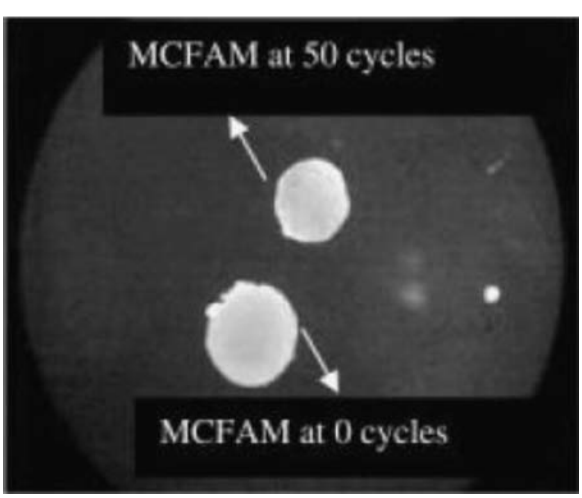


Fig. 7. Optical microscopy profile of microencapsulated coco fatty acid mixture before and after 50 thermal cycles [38].

experiments and simulation. Tests were performed in a packed bed to evaluate the characteristics of encapsulated PCM. Microencapsulation of the PCM was achieved by complex coacervation technique while the performance of the product was evaluated in terms of energy storage and release capacity, hydrophilic properties and encapsulation ratio. It was found that higher coating to paraffin ratio resulted in higher encapsulation ratio of paraffin. The hydrophilicity value of the encapsulated paraffin was found to be dependent on the paraffin to coating ratio with higher ratios leading to less hydrophilicity of the product. From DSC results, the average energy storage capacity was found to be 40–53 J/g. Thermal cycling results showed that the encapsulated paraffin maintained its original geometrical profile even after 1000 thermal cycles (Fig. 5) while the average energy storage capacity (55.38 J/g) changed to 56.09 J/g after 1000 thermal cycles. This shows that the product was able to sustain its energy storage capacity even after 1000 thermal cycles. Moreover, Eulerian granular multiphase model in FLUENT 4.47 was found suitable for such a system.

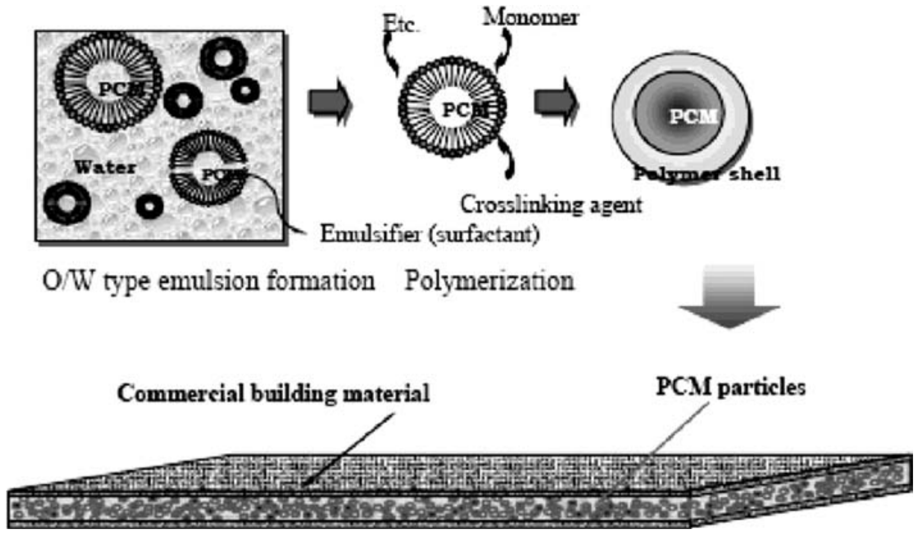


Fig. 8. Concept diagram of building materials containing microencapsulated PCM [41].

Table 6
Various studies on microencapsulated PCM.

	PCM	Shell material	Thermal properties	Method	Capsule size (μm)	Reference
1	*n*-docasane	Polymethylmethacrylate	T_m=41 °C T_f=40.6 °C H_m=54.6 J/g H_f=48.7 J/g	Emulsion polymerization (Fig. 4)	0.16	[37]
2	Paraffin wax	Gelatin + acacia	H_m=20–90 J/g	Coacervation (Fig. 5)		[39]
3	Paraffin wax	Gelatin + acacia (Coating) Gelatin + acacia (Spray)	H_m=193.35–239.78 J/g H_f=196.38–234.05 J/g H_m=145.28–216.44 J/g H_f=148.32–221.52 J/g	Coacervation/spray drying (Fig. 6)		[34]
4	Coco fatty acid	Gelatin + gum Arabic		Coacervation (Fig. 7)	1000	[38]
5	Hexadecane/Octadecane	Melamine-resin	H_m=210 at 23 °C H_m=200 at 24 °C H_m=150 at 28 °C	Insitu polymerization (Fig. 8)	5–20	[41]

The same team prepared microencapsulated PCM particles by complex coacervation and spray-drying methods and studied the performance in terms of encapsulation efficiency and energy storage and release capacity [34]. Test results substantiate that both complex coacervation and spray drying methods could be used to prepare microcapsules of paraffin wax. The microencapsulation efficiency was found to depend on the processing parameters such as core to coating ratio, emulsifying time and the amount of cross-linking agent. It was found to increase with the increase in the amount of cross-linking agent up to 8 ml and homogenizing time up to 10 min while it was found to decrease with the increase in core to coating ratio. SEM micrographs showed that microcapsules are spherical in shape (Fig. 6). In addition, energy storage capacity was found to depend on the core to coating ratio and varied from 145 to 240 J/g. As a result, the prepared microencapsulated paraffin wax was found to be a potential candidate for solar-energy storage applications.

Coacervation technique was used by Ozonur et al. [38] for the successful preparation of microencapsulated PCM from coca fatty acid mixture. The particle size of coco fatty acid microcapsule determined by optic microscope was found to be 1 mm. FT-IR results showed that the chemical stability of coco fatty acid mixture is not affected by microencapsulation. Moreover, the geometric profile of the microencapsulated coco fatty acid mixture was retained even after 50 thermal cycles (Fig. 7). Since the developed microencapsulated PCM was made from cheap materials therefore this was an additional advantage of this study.

Lee et al. [41] developed microencapsulated PCM for building applications (Fig. 8). The microcapsules having average size of 5–20 μm were prepared using in situ polymerization with hexadecane/octadecane as the core and melamine-resin as a shell material. The heat storage capacity of experimental chamber (1.5 m × 1 m × 1 m) was evaluated by applying olefin film with PCM particles having concentration of 100 g/m^2 and thickness of 3 mm and 9 mm respectively. The chamber was heated at 30 °C and then it was allowed to cool. It was found that the thermal energy storage capacity inside the chamber increased with the increase in the thickness of olefin film.

It is worth mentioning here that in most of the research works the performance of microencapsulated PCM has not been extensively compared with that of pure PCM. Therefore, it is suggested that researchers should undertake more comparative research works between pure PCM and microencapsulated PCM so as to evaluate the performance enrichment due to microencapsulation of PCMs. The summary of various studies on microencapsulated PCM incorporated in construction materials and elements is given in Table 6.

4.3.2. *Macroencapsulation*

In this technique, a significant quantity of PCM (up to several liters) can be packed in a container such as tubes, spheres and

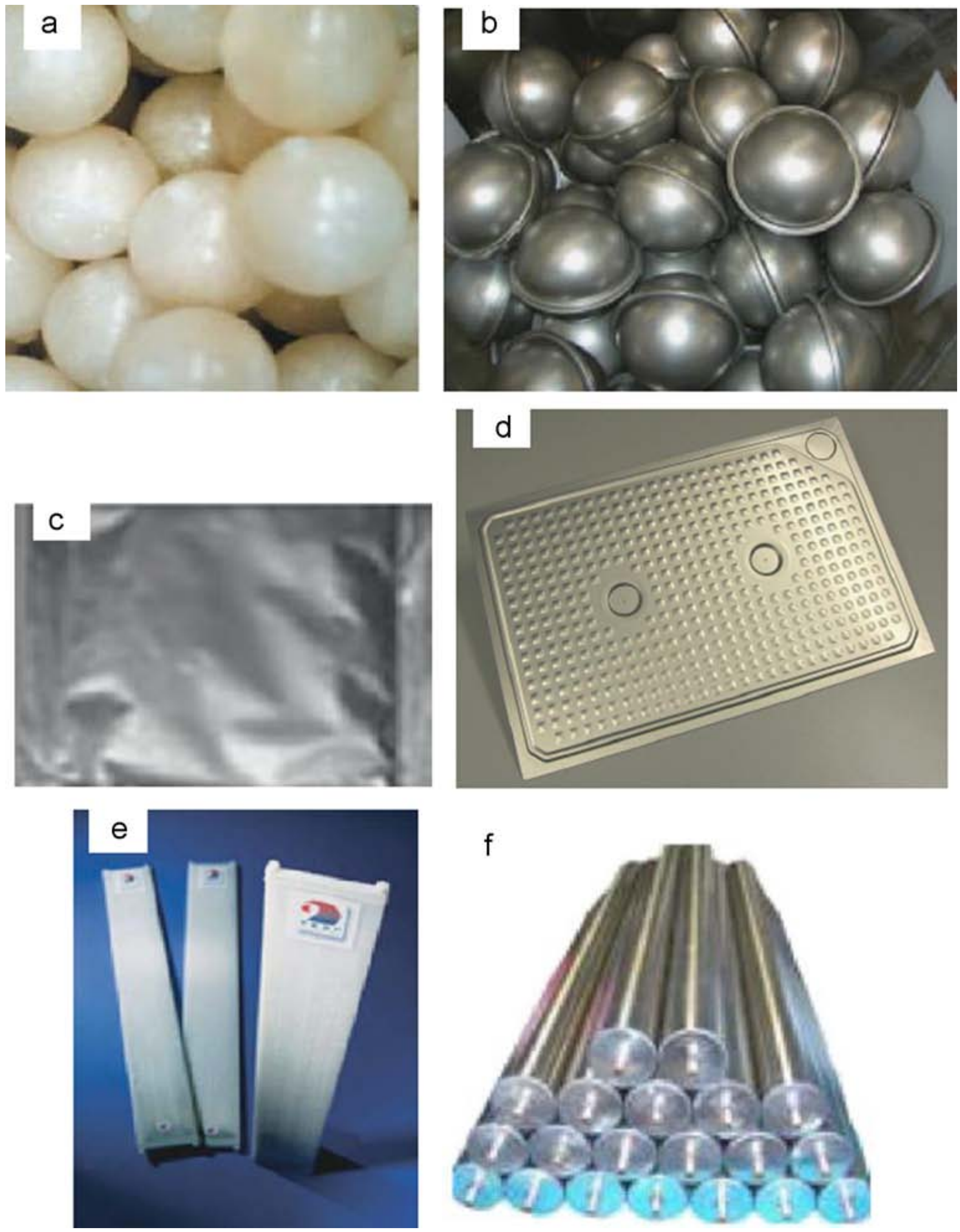


Fig. 9. (a) Metal ball encapsulate (b) Spherical PCM balls (c) PCM in aluminum (d) PCM in aluminum panels (e) PCM in Polypropylene flat panel (f) PCM tube encapsulation [15,43].

panels for subsequent used in construction elements [9]. Macroencapsulation has the following advantages.

(a) Easier to ship and handle.
(b) Can be designed to fit the intended application.
(c) Improves compatibility of PCM with the surrounding by acting as a barrier. However, the container should be compatible with the surrounding.
(d) Reduces external volume changes which are important for building application.

The disadvantages of macroencapsulation include

(a) Poor thermal conductivity.
(b) Have to be protected against destruction (drilling holes or nails in the walls) while the building is in use [42].
(c) More work required at the building site for integration into building structure [42].
(d) Affinity towards solidification at the corners and edges and thereby preventing an effective heat transfer.

Therefore, the encapsulation must be optimized for effective heat transfer rate and at the same time it should be corrosion resistance, thermally stable and reliable. The macroencapsulation is available in various configurations like flat plate, cylinder, shell, tube and spherical (Fig. 9). For details, the readers are referred to [15,17,43].

4.4. Shape-stabilized PCM

In this technique, shape stabilization supports such as high-density polyethylene (HDPE), styrene, and butadiene are used to fabricate shape-stabilized PCM. The PCM and the supporting material are melted and mixed with each other at high temperature followed by cooling the supporting material below the glass

transition temperature until it becomes solid. The shape-stabilized PCM has the following prominent features [11,44,45,46].

(a) Large apparent specific heat.
(b) Appropriate thermal conductivity.
(c) Keeping the shape stabilized during phase transition process.
(d) Thermally reliable (melt/freeze cycle) over a long period.
(e) No need for container.
(f) The mass proportion of PCM can be up to 80%.

Some of the research works focusing on the development of shape stabilized PCM are discussed here.

Inaba and Tu [47] studied the thermophysical properties of shape-stabilized PCM. The shape-stabilized PCM consists of paraffin as thermal storage material and HDPE as a supporting material. Moreover, little quantity of Ethylen-α olein was added to the mixture to reduce oozing rate of the paraffin from the shape-stabilized PCM when subjected to repeated melting/freezing cycles. It was found that the developed shape-stabilized PCM contained 74 wt% paraffin, had a melting temperature of 54.8 °C and heat of fusion 121.5 kJ/kg. The micrograph (Fig. 10) showed that paraffin (black part) was uniformly dispersed in three dimensional netted texture of HDPE (white part) and there was no leakage of the paraffin from the composite even when the paraffin was in the melted state.

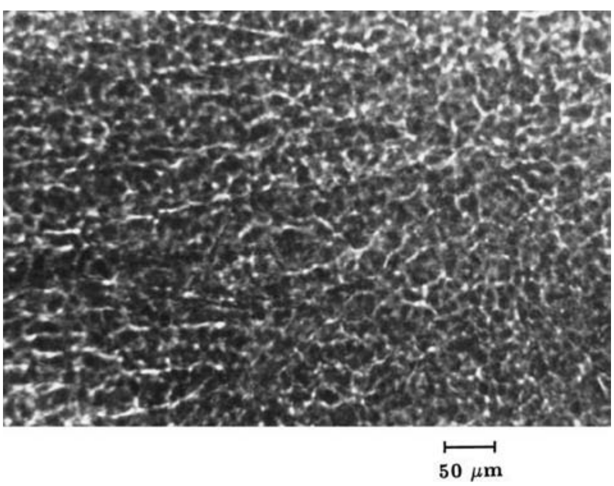


Fig. 10. Micrograph of the shape-stabilized paraffin [41].

For the preparation of shape stabilized PCM (Fig. 11), Ye and Xin-Si [48] selected six types of HDPE having different melt index and density as supporting materials and refined/semi-refined paraffin as thermal storage material. The purpose of selecting HDPE was to obtain shape stabilized PCM having high strength with small percentage of HDPE. Test results showed that shape stabilized PCM with high strength was achieved when the percentage of HDPE was 25–30 wt%. The latent heat of shape stabilized PCM with refined and semi-refined paraffin were found to be 157.04 J/g and 154.73 J/g respectively. This shows that the latent heat of refined as well as semi-refined is almost similar. Therefore, based on the analysis and considering the cost, the semi-refined paraffin was the appropriate choice. It was concluded that the product is cheap, easy to prepare and the latent heat comparable with that of traditional phase change material.

Sari [45] prepared shape stabilized PCM with two different kinds of paraffin (P1 and P2) as latent heat storage material and HDPE as supporting material. From the test results, it was found that paraffin was well dispersed into the network of the solid HDPE (Fig. 12) and the maximum percentage of both types of paraffin retained by HDPE without leakage was found to be 77%. From DSC, the melting temperatures of P1/HDPE and P2/HDPE shape stabilized PCMs were determined as 37.8 °C and 55.7 °C while the latent heats were found to be 147.6 and 162.2 J/g respectively. Furthermore, the thermal conductivity of P1/HDPE and P2/HDPE shape stabilized PCMs increased approximately by 14% and 24% respectively, by the addition of just 3 wt% expanded graphite. It was concluded that the prepared shape stabilized PCMs have great potential for thermal energy storage applications. Moreover, these produced can be cost-effective since they do not require extra encapsulation.

A paraffin/styrene–butadiene–styrene copolymer (SBS) shape stabilized PCM was prepared by Xiao et al. [49]. The shape stabilized product was able to contain up to 80 wt% paraffin. The melting temperature and the heat of fusion of the shape stabilized PCM were found to be 56–58.8 °C and 165.21 kJ/kg respectively. Moreover, the thermal conductivity of the shape stabilized PCM was improved by incorporation of 3% expanded graphite by weight of paraffin/SBS. However, according to Zhang et al. [44], the product has low rigidity i.e. shape stabilized PCM having large volume would not be able to sustain its own weight and will deform.

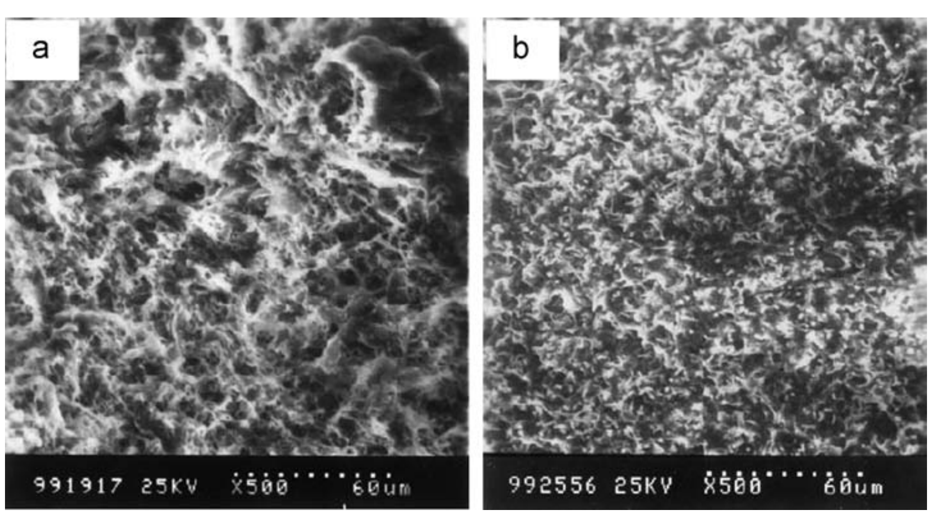


Fig. 11. SEM image of shape-stabilized PCM (a) with refined paraffin (b) semi-refined paraffin [48].

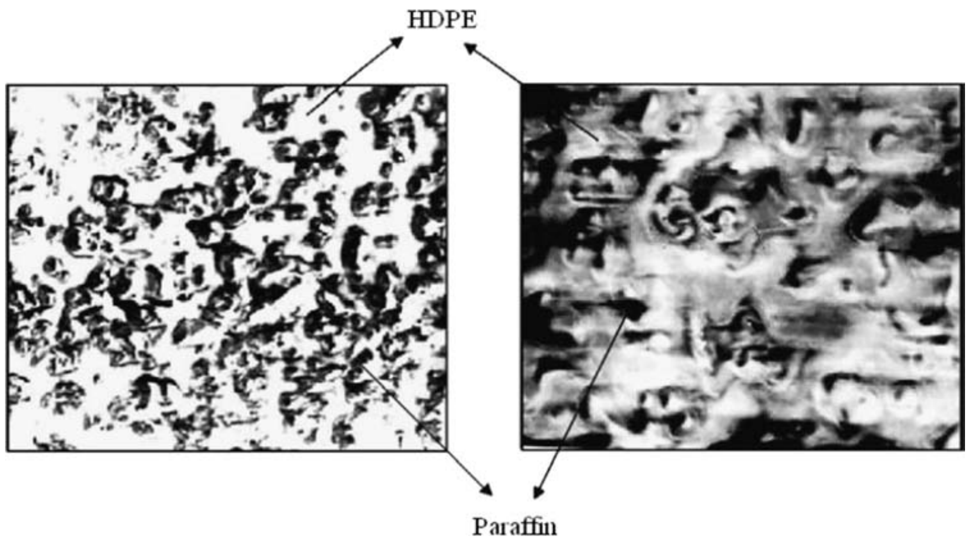


Fig. 12. SEM image of shape-stabilized Paraffin/ High density polyethylene [45].

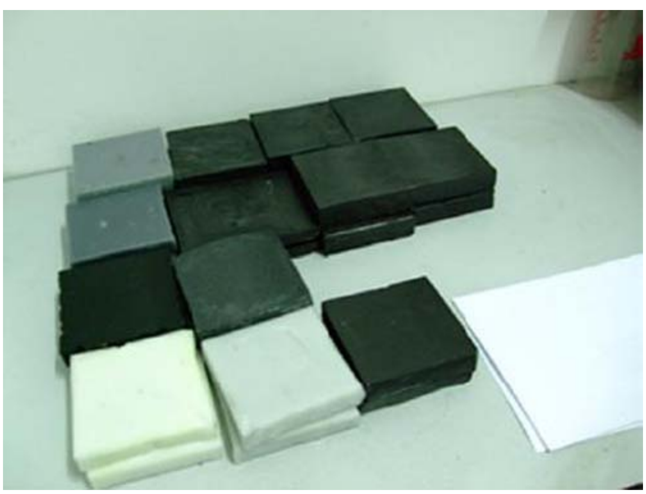


Fig. 13. Photo of shape-stabilized Paraffin/ High density polyethylene [50].

The thermal conductivity of the shape stabilized paraffin/HDPE was improved by Cheng et al. [50] by incorporation of graphite powder and expanded graphite (Fig. 13). The results showed that the thermal conductivities of the shape stabilized PCM with expanded graphite were greater than the shape stabilized PCM with graphite powder. With the addition of up to 4.6 wt% expanded graphite, the improvement in thermal conductivity was more than four times than without expanded graphite. The latent heat values decreased little by incorporation of additives, however, the melting temperature of the shape stabilized PCM approached that of pure paraffin with a standard deviation of $\pm$ 1.1 °C.

From the above discussion, it can be concluded that shape stabilized PCM is a promising technique and should be studied future with focus on its application especially in buildings. The summary of research work on shape-stabilized PCM is given in Table 7.

4.5. *Form-stable composite PCM*

In literature the terms form-stable and shape-stabilized PCMs have been used interchangeably [45]. However, for this review, the term form-stable composite PCM is used to define a composite PCM which retain an optimum/maximum percentage of PCM and shows no sign of leakage when the temperature of the composite is above the melting point of PCM. Also, it is not necessary for the supporting material in form-stable composite PCM, as opposed to shape-stabilized PCM, to melt [51–53].

The form-stable composite PCM can be obtained by natural immersion (as discussed in Section 4.2) or vacuum impregnation. The natural immersion is simple and easy to use. However, the retention capacity of building materials to store thermal energy is low. Therefore, the retention capacity of porous building materials can be increased through vacuum impregnation method [54]. Various vacuum impregnation equipment have been used to prepare the form-stable composite PCM. One of them is shown in Fig. 14 [55].

In review papers on thermal energy storage using PCM, the literature on form-stable composite PCM is scarce. Therefore, a detailed analysis of the work done by various researchers is presented here.

4.5.1. *Diatomite as supporting material for PCM*

Diatomite is the skeletal remains of single celled plants called diatoms, hence the name diatomite. Diatomite finds its application in many fields such as a construction material, heat, cold and sound insulator, filler absorbent, abrasive, and ingredient in medicine [56]. Furthermore, due to its highly porous microstructure, high absorptivity and inertness, it is being used as a supporting material for storing PCM [56–59]. According to the World mineral production report by the British geological survey, the total worldwide production of diatomite in 2011 was around 2.68 million metric tonnes with Argentina, USA, China and Japan, appearing as the major producer having production capacity of 1, 0.6, 0.44 and 0.1 million metric tonnes and representing a share of around 80% of the total worldwide production [60]. Some of the prominent works by various researchers on diatomite as supporting materials for PCM are presented in subsequent paragraphs.

Xu and Li [58] evaluated the thermal energy storage performance of cement-based composite (TESC) by incorporation of paraffin/diatomite form-stable composite PCM (Fig. 15). The maximum percentage of paraffin retained by diatomite powder (DP) through direct incorporation technique was found to be 47.4 wt%. From DSC analysis, the melting temperature and latent heat of the composite PCM was found to be 41.11 °C and 70.51 J/g. The paraffin/diatomite composite PCM was then incorporated, in replacement mode, in cement-based composite at 10, 15, 20, and

Table 7
Various studies on shape-stabilized PCMs.

	PCM	Supporting Material	Combination	Thermal properties	Reference
1	Paraffin (Pentacosane)	High density polyethylene (HDPE)	Paraffin/HDPE (74/26) (Fig. 10)	T_m=54.15 °C H_m=121.4 J/g	[47]
2	Paraffin	High density polyethylene	Paraffin/HDPE (75/25) (Fig. 11)	Refined H_m=157.04 J/g Semi refined H_m=154.73 J/g	[48]
3	Paraffin	Stryrene–butadiene–styrene (SBS)	Paraffin/SBS (80/20)	T_m=56–58 °C	[49]
4	Paraffin	High density polyethylene	Paraffin/HDPE (77/23) (Fig. 12)	Paraffin1 (T_m=37.8 °C H_m=147.6 J/g) Paraffin2 (T_m=55.7 °C H_m=162.2 J/g)	[45]
5	Paraffin	High density polyethylene	Paraffin/HDPE (80/20) (Fig. 13)	T_m=43.29 °C H_m=107.93 J/g	[50]

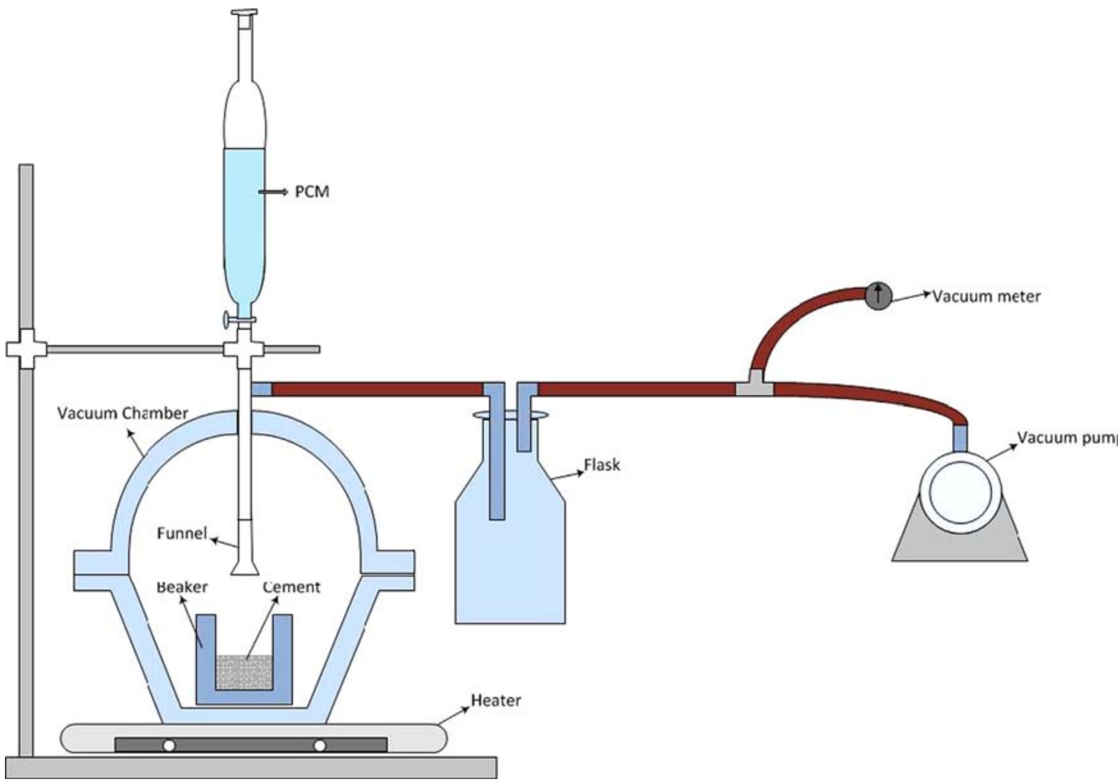


Fig. 14. Schematic of vacuum impregnation system [55].

30% by weight of cement. Test results showed that in comparison to control normal cement-based composite, the incorporation of paraffin/diatomite composite PCM into cement-based composite reduced the 28-days compressive and flexural strength, drying shrinkage strain and thermal conductivity by 48.7%, 47.5%, 80.7% and 33.6% respectively. From thermal performance test, it was found that TESC panel ($200 \times 100 \times 15$ mm^3) with 30 wt% paraffin/diatomite composite PCM reduced the temperature at the inner surface of the panel and inside the wooden box. Therefore, testifying the thermal energy storage performance of TESC with paraffin/diatomite composite PCM.

Karaman et al. [56] prepared polyethylene glycol/diatomite composite PCM through vacuum impregnation technique. Through this technique, the maximum percentage of polyethylene glycol confined into the pores of diatomite was found to be 50 wt%. For the composite PCM, the melting temperature and latent heat determined by DSC were found to be 27.7 °C and 87.09 J/g. Thermal cycling test indicated that the composite PCM is thermally and chemically reliable when subjected to 1000 melting and freezing cycles. From the TG curve, it was found that the composite PCM has good thermal stability. Furthermore, the thermal performance test on small test room $100 \times 100 \times 100$ mm^3 was also carried out. In comparison to control room (without composite PCM), the composite PCM room successfully reduced the indoor center temperature by 1.01 °C. Thus, the composite PCM was found to be a promising candidate for thermal energy storage applications in buildings.

4.5.2. Expanded perlite as supporting material for PCM

Perlite, an amorphous volcanic glass, is one of the nature's most versatile and efficient minerals having relatively high water content. When this amorphous volcanic glass is heated rapidly at 850–1150 °C, it expands up to 10–20 times its original volume [61,62] due to vaporization of combined water. The resulting product, expanded perlite, has unique characteristics such as lightweight, highly porous, and high fire resistance. which makes it a first-class choice for diverse applications such as thermal energy storage applications, construction, filtration, horticulture, industrial, and insulation. According to the World mineral production statistics, Greece, China, Iran, Turkey, USA and Japan are the major perlite producers. In 2011, these countries produced 0.7, 0.7, 0.55, 0.429, 0.4, and 0.3 million metric tonnes respectively [60]. Various researchers have successfully utilized expanded perlite as supporting material for PCM [52,63]. These works are presented herein.

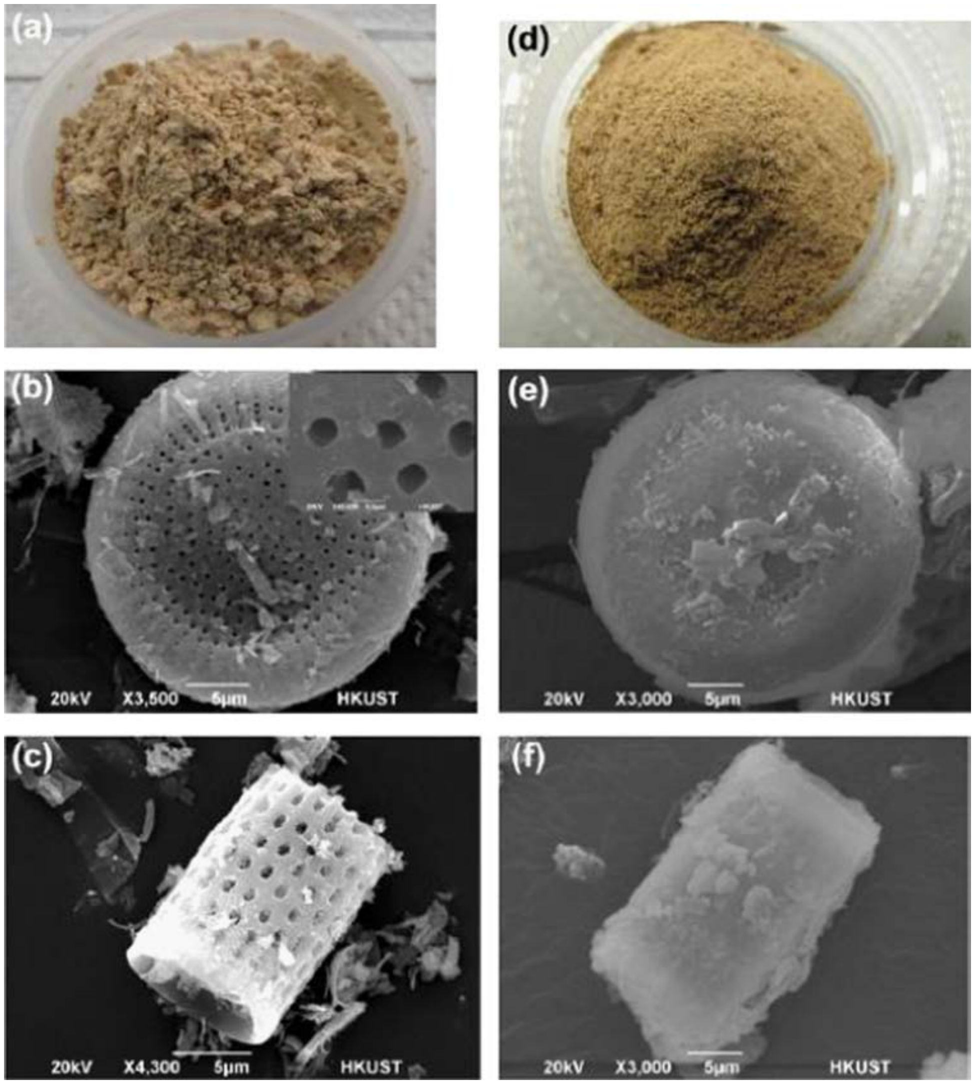


Fig. 15. Morphologies of DP and paraffin/DP composite PCM in both macro and microscales: (a) DP; (b and c) SEM morphologies of DP in disc-like and cylindrical shapes, respectively; (d) paraffin/DP composite PCM; (e and f) SEM morphologies of paraffin/DP composite PCM in disc-like and cylindrical shapes, respectively [58].

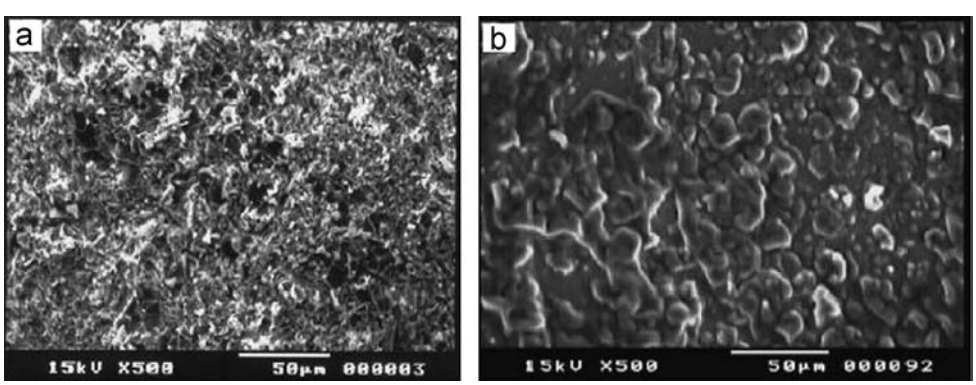


Fig. 16. SEM micrographs of EP (a) before loading lauric aicd (b) after loading lauric acid [63].

Sari et al. [63] successfully incorporated 60 wt% of lauric acid into expanded perlite (EP) through vacuum impregnation technique (Fig. 16). The composite PCM showed large enthalpy of 93.36 J/g and suitable melting temperature of 44.13 °C. Thermal cycling test revealed that the composite PCM has good thermal and chemical reliability after 1000 melting/freezing cycles. The thermal conductivity of the composite PCM was enhanced by incorporating 10% by weight of expanded graphite into the composite. Based on the test results, it was concluded that the composite PCM is a promising contestant for thermal energy storage applications.

Sari and Karaipekli [52] made form-stable composite PCM through vacuum impregnation by using capric acid as PCM and expanded perlite as supporting material. The PCM was confined in maximum percentage of 55 wt% without leakage of the melted PCM from the porous structure of expanded perlite. The melting temperature and latent heat of composite PCM determined by DSC

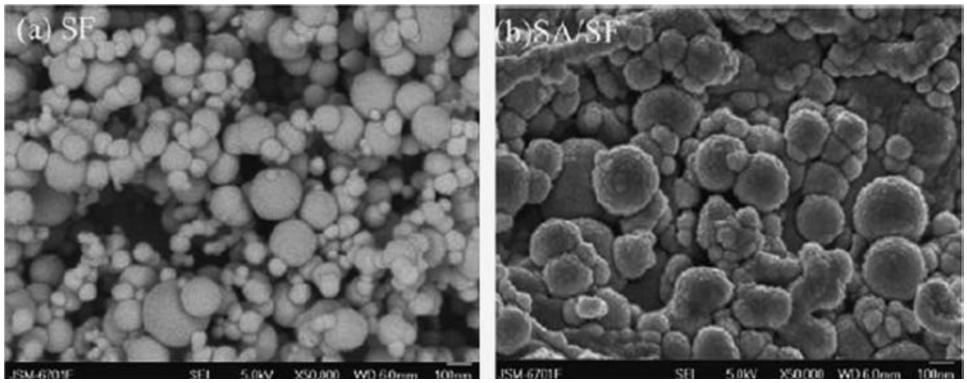


Fig. 17. SEM micrographs of SF and SA/SF composite PCM [67].

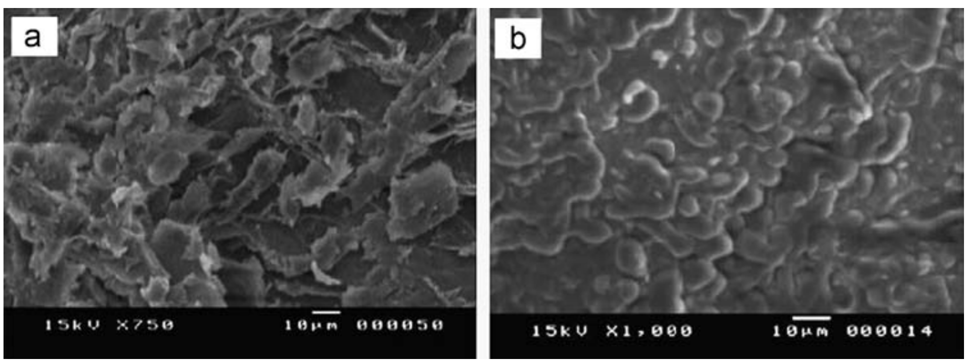


Fig. 18. SEM images (a) VMT (b) form-stable CA-MA/VMT composite PCM [53].

were found to be 31.8 °C and 98.1 J/g. The changes observed in the thermal properties after 5000 thermal cycles were less than ± 10%. Moreover, the composite PCM showed 64% increase in thermal conductivity by the addition of 10% expanded graphite. From test results, it was concluded that the composite PCM can be used to improve indoor thermal comfort.

Sari et al. [57] also experimental investigated the suitability of fatty acid esters-based composite PCM for thermal energy storage applications in buildings. The composite PCM was obtained by direct incorporation of erythritol tetrapalmitate (ETP) and erythritol tetrastearate (ETS) into diatomite and expanded perlite. The maximum percentage of PCM retained by diatomite and expanded perlite through capillary and surface tension forces was found to be 57 and 62 wt% respectively. DSC results showed that the thermal properties (melting temperature 19.64–30.15°C and latent heat 110.6–119.19 J/g) of the composite PCM are suitable for thermal energy storage applications in buildings. The composite PCM was found to be thermally and chemically reliable when subjected to 1000 thermal cycles. Also, the composite PCM was found to be thermally stable in the working temperature range. Furthermore, 5 wt% incorporation of expanded graphite into composite PCM showed the best results in terms of increase in thermal conductivity values (57–73%) and decrease in the amount of latent heat storage capacity.

4.5.3. Expanded graphite as supporting material for PCM

The term graphite, an allotrope of carbon, was coined by Abraham Gottlob Werner in 1789. Expanded graphite is prepared from natural graphite through chemical oxidation in the presence of concentrated sulfuric acid/nitric acid/mixture of sulfuric and nitric acid, followed by drying up process in the oven and finally by rapid heating in a furnace at high temperature (e.g. 900 °C) [36]. It has good absorption ability and high thermal conductivity. Therefore, it has been used in thermal energy storage applications as a supporting material for PCM as well as to improve the thermal conductivity of the system [64–66]. According to the literature, the world total production of graphite, in 2011, was around 2.1 million metric tonnes with China having a share of around 1.8 million metric tonnes representing almost 86% of the world total [60]. Various researchers have successfully utilized expanded graphite as supporting material for PCM. Some of the prominent research works are presented herein.

Sari et al. [64] prepared palmitic acid/expanded graphite composite PCM for latent heat thermal energy storage applications. Through vacuum impregnation technique, palmitic acid was confined into the pores of expanded graphite by 80 wt%. FT-IR results showed the interaction between palmitic acid and expanded graphite is physical in nature. The phase change properties i.e. the melting temperature and latent heat for the composite PCM were found to be as 60.88 °C and 148.36 J/g. Thermal cycling test showed that the changes observed in the thermal properties and chemical structure of composite PCM after 3000 melting/freezing cycles are very little and in the acceptable range. Furthermore, the thermal conductivity of the composite PCM was increased by 2.5 times than pure palmitic acid with addition of 20% expanded graphite. Based on the test results, it was concluded that the composite PCM has considerable potential for solar latent heat thermal energy storage applications.

Wang et al. [66] incorporated 90 wt% of polyethylene glycol into expanded graphite using the direct incorporation technique. FT-IR results showed that the composite PCM is chemically compatible. The melting temperature, enthalpy and thermal conductivity of the composite PCM were found to be 61.47 °C, 161.2 J/g and 1.324 $Wm^{-1}K^{-1}$ respectively. The changes experienced in thermal properties by the composite PCM after 100 thermal cycles

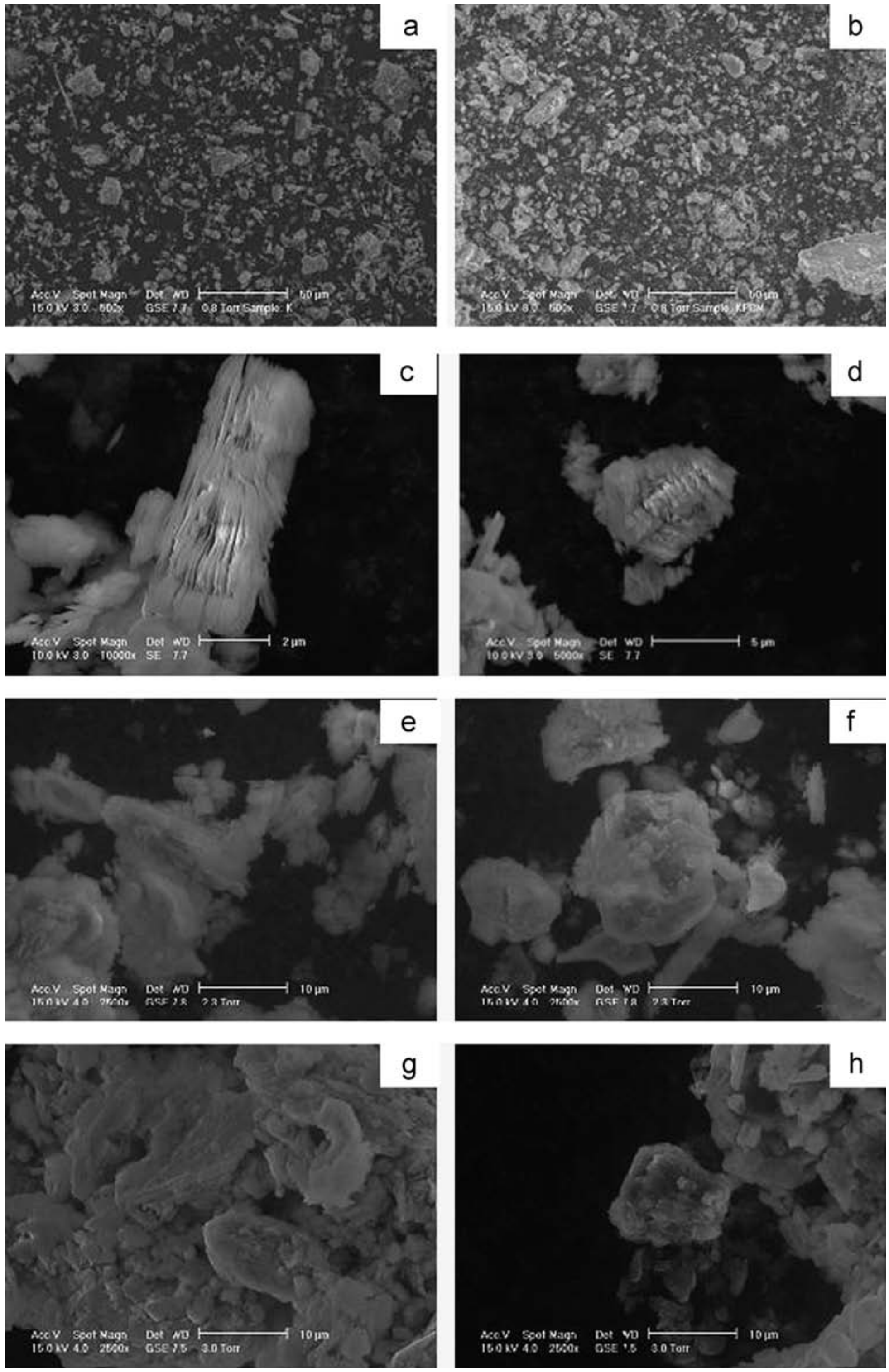


Fig. 19. ESEM morphologies at microscale (a) KO powder; (b) LA-KO composite PCM powder; (c and d) KO in lamellar shape; (e–h) LA-KO composite PCM [75].

were less than 2.5%. Thus, polyethylene glycol/expanded graphite composite PCM with the large latent heat and high thermal conductivity was found to be a promising candidate for latent heat storage applications.

4.5.4. Silica fume as supporting material for PCM

Silica fume, also known as volatilized silica, microsilica or condensed silica fume, is produced by electric arc furnace as a by-product in the production of silicon and ferrosilicon alloy [67]. This ultra fine powder, with an average diameter of 0.1 μm, finds its main application as pozzolanic material for high performance concrete. According to the literature, the by-product from the production of ferrosilicon alloy with 50% silicon contains much lower silica content and therefore is unsuitable for use as a pozzolanic material [68]. Huge amount of this low silica content silica fume is produced around the world and because of high purification cast this product is usually dumped in open fields

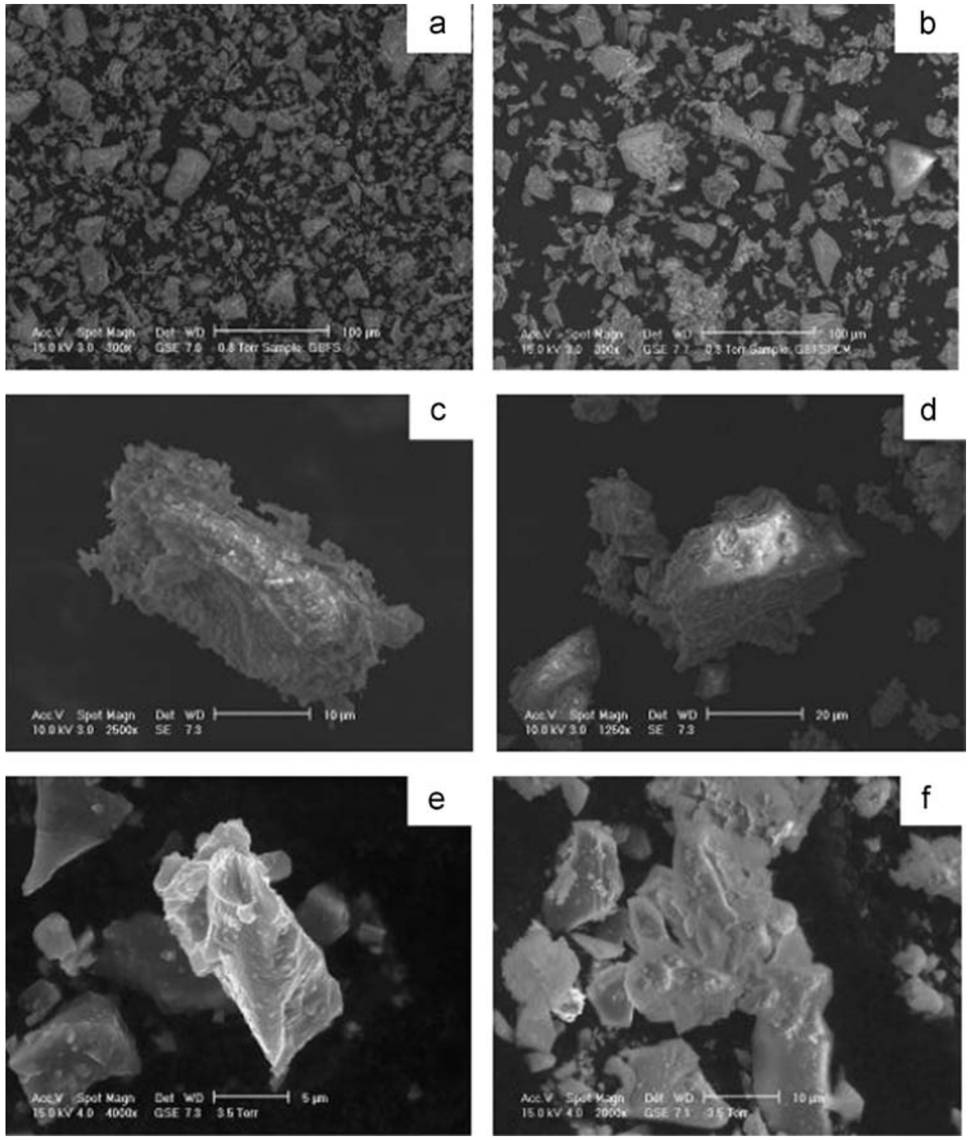


Fig. 20. ESEM morphologies at microscale (a) GGFS powder; (b) LA-GGFS composite PCM powder; (c and d) GGFS particles shape; (e and f) LA-GGFS composite PCM [79].

causing serious dust pollution and associated health problems [122]. Moreover, both low and high silica content silica fume have nano porous structure and have been used in thermal storage applications as supporting material for PCM.

Wang et al. [67] successfully loaded 47 wt% stearic acid (SA) into silica fume (SF) matrix through vacuum impregnation technique. SEM micrographs showed that stearic acid is held by silica fume through hydrogen bonds (Fig. 17) while the FT-IR investigation showed that the interaction between stearic acid and silica fume is physical in nature. The composite as form-stable thermal storage material melted at 58.8 °C with a latent heat of 82.53 J/g. Thermal cycling test indicated that the composite PCM has good thermal and chemical reliability after 600 melting/freezing cycles.

4.5.5. Vermiculite as supporting material for PCM

Vermiculite is a naturally occurring phyllosilicates formed from various parent rock minerals generally as the result of weathering. It is formed from the layer of silicate and aluminate minerals that produce 2:1 lamellar structure i.e. 2 tetrahedral sheets for every one octahedral sheet [69]. This material is abundantly available in nature and according to the literature, in 2011; South Africa, China, USA and Brazil were the major producers with a share of 0.17, 0.13, 0.1 and 0.05 million metric tonnes respectively [60]. It is porous, cheap, lightweight, and find applications in construction, thermal insulation, thermal energy storage, agriculture, horticulture, etc. [53].

Karaipekli and Sari [53] prepared a form-stable composite PCM by incorporating capric-myristic acid (CA-MA) into grinded vermiculite (VMT). They were able to successfully retain 20% by weight into vermiculite without seepage of PCM from the composite (Fig. 18). The composite showed excellent thermal and chemical reliability when subjected to 3000 cycles of melting and freezing. As per the authors, the composite mixture can be successfully utilized into mortar and concrete.

4.5.6. Kaolin as supporting material for PCM

The word Kaolin is derived from the name of the Chinese town Kao-Ling (Gaoling), located in the Jiangxi Province of southeast China [70]. Kaolin or China clay is a geological term referring to a rock that is rich is Kaolinite. Kaolinite is a hydrated aluminum ($SiO4$) tetrahydral sheet linked to one alumina [Al (O, OH)6] octahedral sheet through the sharing of apical oxygen′s [71,72].

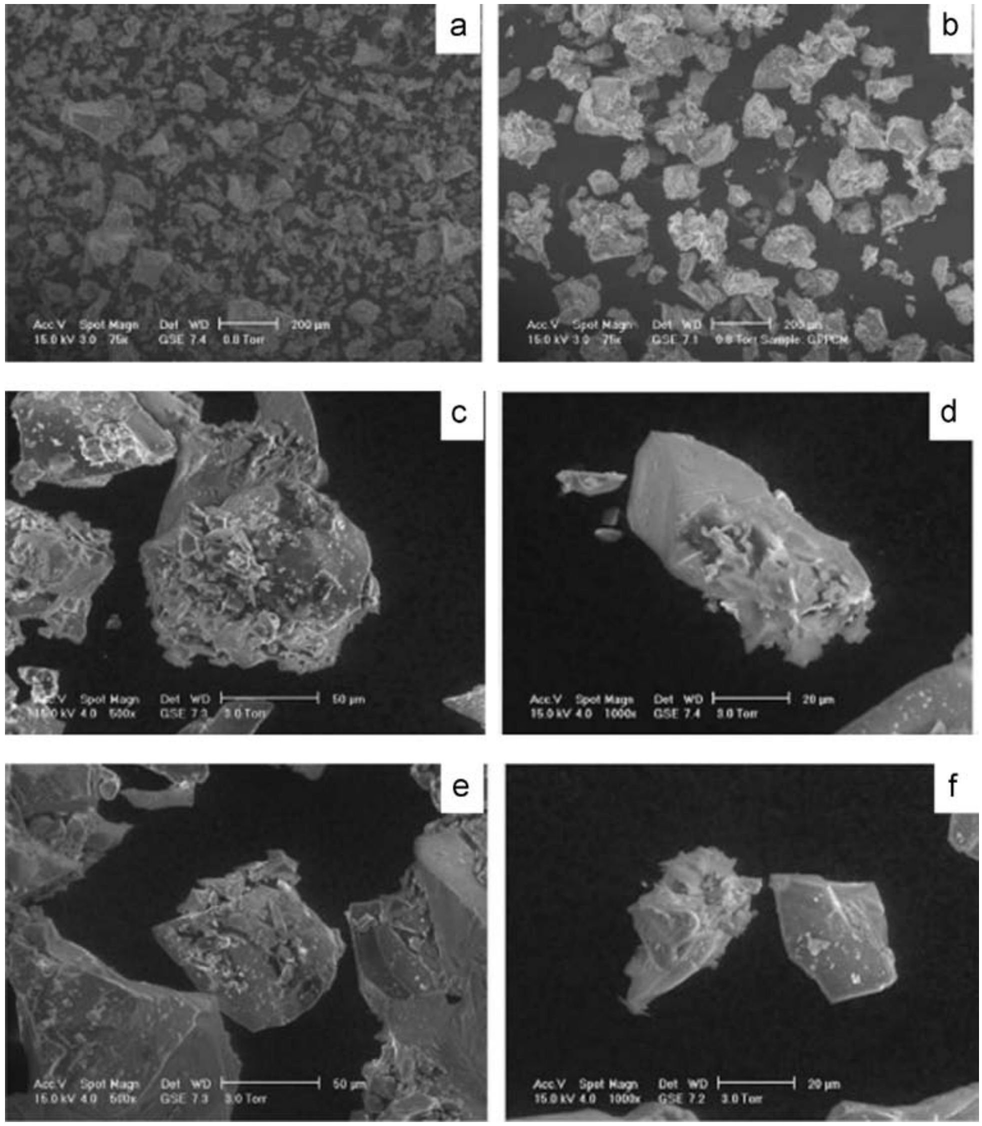


Fig. 21. ESEM images (a) GP and (b–f) *n*-octadecane-GP composite [83].

Kaolin has a wide range of industrial applications, mostly dominated by paper and ceramic industry followed by specialty applications such as fillers in paints and rubber [73] and has also been used extensively in mortar and concrete to improve its strength and durability [74]. According to the British Geological Survey [60], the world total Kaolin production in 2011 was around 25.7 million tonnes with USA, Germany, China, Brazil, Iran, Korea and UK as the major producers. These countries produced more than 19.0 million metric tonnes representing around 75% of the world total production.

Memon et al. [75] developed novel form-stable composite PCM having excellent heat transfer control in terms of thermal storage, thermal stability and reliability, physical and chemical compatibility by incorporation of Lauryl alcohol (LA) into Kaolin (KO) through vacuum impregnation. The maximum fraction of LA retained in KO through this technique was 24 wt%. Therefore, this composite was characterized as form-stable composite PCM. SEM images showed that LA was held by the porous and layered structure of KO due to the effect of capillary and surface tension forces which, in turn, prevented the seepage of the melted PCM (Fig. 19). FT-IR results indicated that the form-stable composite has good chemical stability and the interaction between LA and KO is physical. The melting temperature and latent heat of the form-stable composite were measured as 19.14 °C and 48.08 J/g by DSC analysis. TGA and thermal cycling test revealed that the form-stable composite is thermally stable and reliable. The thermal performance test on small scale showed that in comparison to cement paste panels without composite PCM, the form-stable composite PCM panels were effective in reducing the indoor center temperature by 4 °C. It was therefore concluded that the prepared form-stable composite is a promising candidate for thermal energy storage in buildings. In addition, apart from wide range industrial applications of kaolin, its utilization for the purpose of thermal storage in buildings open a new venture for kaolin industry of the world.

4.5.7. Granulated blast furnace slag as supporting material for PCM

Ground granulated blast furnace slag (GGBS) is a by-product of iron and steel making in a blast furnace where iron ore, lime stone and coke are heated at a temperature of around 1500 °C. When these raw materials melt in the blast furnace, it produces molten iron and molten slag. Molten slag, which is lighter and floats on the top of molten iron, is rapidly chilled with high pressure water jet to obtain granular particles. These granular particles are then dried and ground into fine powder to obtain a product that is

known as GGBS [76]. GGBS is a well known construction material and is being successfully used to produce blended cements, mortar and concrete [77]. Utilization of GGBS in concrete results in improved workability, increased strength and durability, high resistance to sulfate attack and alkali–silica reaction, low heat of hydration, superior architectural appearance etc. Its use in concrete is recognized by LEED (Leadership in Energy and Environmental Design) as improving the sustainability of the project [78]. According to the literature [78], its use in concrete climbed to 7 million tonnes. Considering all these benefits, GGBS is a potential candidate for thermal energy storage in buildings.

Memon et al. [79] developed form-stable composite phase change material by incorporating Dodecyl alcohol (DA) into GGBS through vacuum impregnation. The maximum percentage of DA retained in GGBS without seepage was 11 wt% (Fig. 20). FT-IR results validate that the components of the form-stable composite are chemically stable. The melting temperature and latent heat of the form-stable composite as measured by DSC were found to be 21.16 °C and 22.51 J/g. The results of TGA and thermal cycling test confirmed that the form-stable composite is thermally stable and reliable. It was therefore concluded that the prepared form-stable composite is a potential candidate for thermal energy storage in buildings. According to the authors, the utilization of this material for the purpose of thermal storage in buildings will open a new venture for GGBS industry of the world. It was suggested that the compatibility of form-stable composite PCM with cement should be checked so that it can be successfully utilized in walls of buildings made with mortar and concrete. In addition, the mechanical performance and durability aspects of the mortar/concrete prepared with DA-GGBS composite should also be studied.

4.5.8. Waste glass as supporting material for PCM

Discarded waste glass is one of the major contributors of solid waste. It has become a significant burden on the landfills throughout the world. United Nation estimates the volume of yearly disposed glass waste to be 14 million tonnes [80]. In Hong Kong, around 100,000 tonnes of glass containers are disposed in landfills every year [81]. Moreover, glass is not biodegradable. Therefore, landfills do not offer environmental friendly solution to its disposal. In addition, due to the lack of a local manufacturing industry to serve as a possible recycling outlet, disposal and recycling of waste glass have become a major challenge for Hong Kong [81,82]. In order to save landfills for useful applications, it is vital to find a sustainable solution to reuse waste glass.

Memon et al. [83] investigated the feasibility of using soda-lime waste glass powder for latent heat storage application. *n*-octadecane was loaded into glass powder (GP) (Fig. 21). The surface morphology, chemical compatibility, phase change behavior, thermal stability and reliability were determined using Scanning electron microcope, Fourier transformation infrared spectrum analysis, Differential scanning calorimetry, Thermo gravimetric analyzer and thermal cycling test. The thermal performance of cement paste composite PCM was also evaluated. The maximum mass percentage of *n*-octadecane retained by GP was found to be 8. FT-IR results showed that the interaction between the components of composite PCM is physical in nature. The melting and freezing temperatures of the composite PCM were found to be 26.93 °C and 25.03 °C while the latent heat of melting and freezing were 18.97 J/g and 18.95 J/g. TGA and thermal cycling results confirmed that the composite PCM is thermally stable and reliable. Thermal performance test showed that the cement paste panel with composite PCM reduced the indoor temperature by 3 °C. It was concluded that the composite PCM can be used for thermal energy storage applications in buildings. Moreover, its usage will provide sustainable solution to reuse the waste glass. Thus, landfills can be saved for useful applications.

4.5.9. Other supporting materials for PCM

Chen et al. [84] prepared form-stable composite PCM by incorporation of *n*-octadecane within molecular sieve 5 A. The maximum percentage of *n*-octadecane retained by molecular sieve was determined as 33.3 wt%. From DSC analysis, the melting temperature and latent heat were found to be 28.33 °C and 101.14 J/g. In addition, the composite PCM showed improved thermal stability due to the synergistic effect between the components.

Li et al. [85] through vacuum impregnation incorporated mixture of capric-palmitic acid into attapulgite. The PCM was held by the layered and laminated structure of attapulgite with the composite PCM containing 35 wt% showing no sign of leakage. FT-IR results showed that the components of composite PCM are chemically compatible and the interaction between them is physical in nature. The composite PCM melted at 21.7 °C and possessed latent heat of 48.2 J/g

Karaipekli and Sari [86] experimentally investigated the suitability of fatty acid esters-building materials as novel form-stable composite PCM for thermal energy storage applications in buildings. The composite PCM was obtained by vacuum impregnation of erythritol tetrapalmitate and erythritol tetrastearate into cement and gypsum and the maximum percentage of esters retained by cement and gypsum were found to be 18 and 22 wt% respectively. DSC results showed that the thermal properties (melting temperature 21.6–32.3 °C and latent heat 35.9–43.3 J/g) of the composite PCM are suitable for thermal energy storage applications in buildings. The composite PCM was found to be reliable even when it was subjected to 1000 thermal cycles. TG analysis showed that the composite PCM is thermally stable. Based on the test results, it was concluded that the prepared composite PCM is a promising candidate for thermal energy storage application in buildings.

From analysis of this section, it can be seen that most of the researchers have focused on the development of form-stable composite PCM. Therefore, it is suggested that in future, researchers should also focus on applied investigation of form-stable composite PCM. The summary of various studies on form-stable composite PCM is presented in Table 8.

5. Measurement of thermal properties of PCM/composite PCM

The performance of a thermal energy storage system is directly associated with the phase change properties of PCM. It has been pointed out [24] that the data supplied by the producers could be incorrect, doubtful and over optimized. Therefore, it is necessary to make measurements so as to get the correct phase change properties of PCM. Several measurement techniques such as Differential Scanning Calorimetry, Differential Thermal Analysis, and T-history method exists, however, DSC is the most common one and therefore would be extensively discussed.

5.1. Differential scanning Calorimetry (DSC)

5.1.1. Introduction

Differential Scanning Calorimetry is an analytical technique developed by Watson et al. in 1962 [87]. The term was coined to describe equipment having the capability to directly measure the energy and allow accurate measurement of heat capacity [88]. DSC measures the temperatures and heat flows associated with material changes as a function of time and temperature in a controlled environment [89,90]. The measurements provide qualitative and quantitative data about physical and chemical changes that

Table 8
Various studies on form-stable composite PCM.

	Container	PCM	% Retained	Thermal properties	References
1	Diatomite	Erythritol tetra palmitate	57	T_m = 19.6 °C T_f = 14.3 °C H_m = 110.6 J/g H_f = 101.2 J/g	[57]
		Erythritol tetra stearate		T_m = 29.8 °C T_f = 30 °C H_m = 116.1 J/g H_f = 114.8 J/g	
	Expanded perlite	Erythritol tetra palmitate	62	T_m = 19.8 °C T_f = 14.4 °C H_m = 119 J/g H_f = 111.5 J/g	
		Erythritol tetra stearate		T_m = 30.1 °C T_f = 30 °C H_m = 119.1 J/g H_f = 128.6 J/g	
2	Diatomite	Paraffin	47.4	T_m = 41.11 °C T_f = 47.54 °C H_m = 70.51 J/g H_f = 71.96 J/g	[58]
3	Diatomite	Polyethylene glycol	50	T_m = 27.70 °C T_f = 32.19 °C H_m = 87.09 J/g H_f = 82.22 J/g	[56]
4	Diatomite	Decanoic/Dodecanoic		T_m = 16.74 °C H_m = 66.8 J/g	[59]
5	Expanded perlite	Lauric acid	60	T_m = 44.13 °C T_f = 40.97 °C H_m = 93.36 J/g H_f = 94.87 J/g	[63]
6	Expanded graphite	Palmitic acid	80	T_m = 60.88 °C T_f = 60.81 °C H_m = 148.36 J/g H_f = 149.66 J/g	[64]
7	Expanded graphite	Polyethylene glycol	90	T_m = 61.46 °C H_m = 162.2 J/g	[66]
8	Silica fume	Stearic acid	47	T_m = 59.9 °C T_f = 54.7 °C H_m = 82.53 J/g H_f = 84.47 J/g	[67]
9	Molecular sieve	*n*-octadecane	33.3	T_m = 28.3 °C T_f = 26.8 °C H_m = 101.1 J/g	[84]
10	Vermiculite	Capric + Myristic acid	20	T_m = 19.8 °C T_f = 17.1 °C H_m = 27 J/g	[53]
11	Kaolin	Lauryl alcohol	24	T_m = 19.14 °C H_m = 48.08 J/g	[75]
12	Ground granulated blast furnace slag	Dodecyl alcohol	11	T_m = 21.16 °C T_f = 19.1 °C H_m = 22.51 J/g H_f = 21.62 J/g	[79]
13	Glass powder	*n*-octadecane	8	T_m = 26.93 °C T_f = 25.03 °C H_m = 18.97 J/g H_f = 18.95 J/g	[83]
14	Attapulgite	Capric-palmitic acid	35	T_m = 21.7 °C H_m = 48.2 J/g	[85]
15	Cement	Erythritol tetra palmitate	18	T_m = 21.9 °C T_f = 14.5 °C H_m = 37.2 J/g H_f = 38.1 J/g	[86]
		Erythritol tetra stearate		T_m = 32.2 °C T_f = 29.8 °C H_m = 35.9 J/g H_f = 36.1 J/g	
	Gypsum	Erythritol tetra palmitate	22	T_m = 21.6 °C T_f = 14.5 °C H_m = 42.3 J/g H_f = 45.9 J/g	
		Erythritol tetra stearate		T_m = 32.3 °C T_f = 29.5 °C H_m = 43.3 J/g H_f = 44.4 J/g	

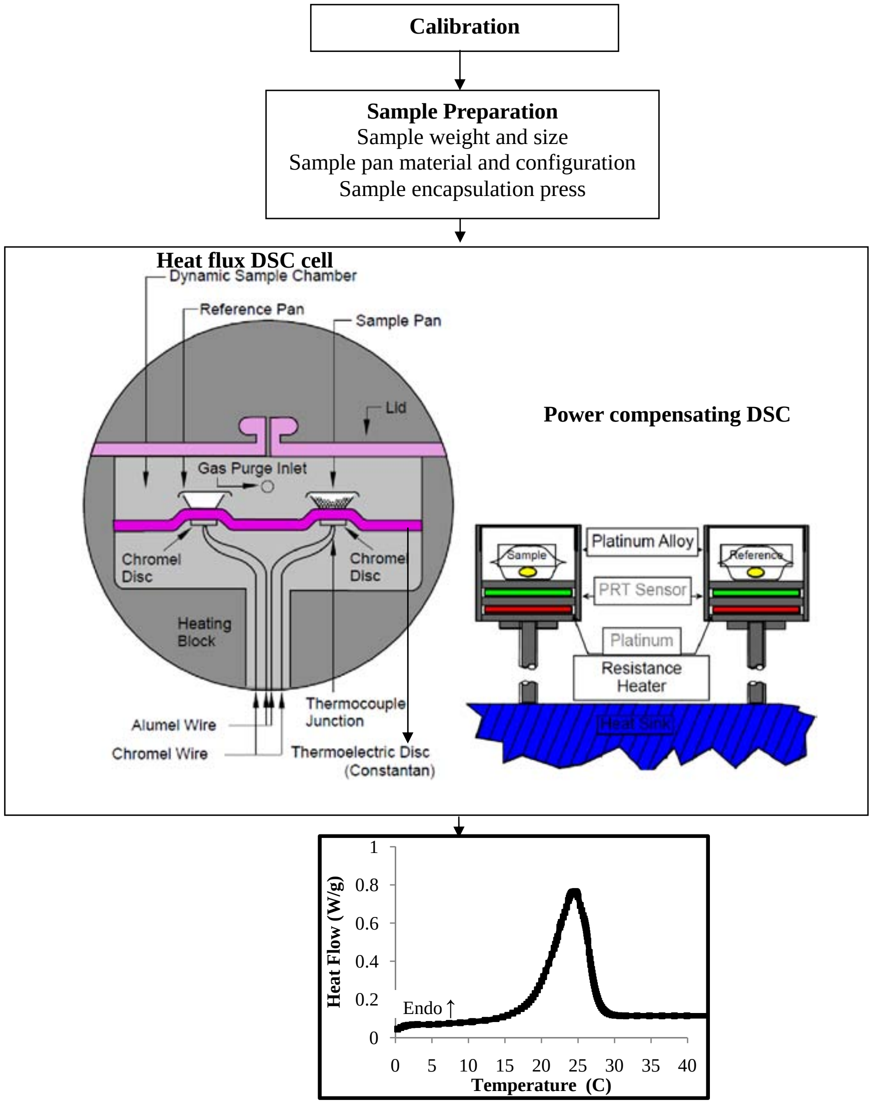


Fig. 22. DSC analysis protocol {DSC heat flux and power compensating cell from references [91,92]}.

involve endothermic or exothermic processes [90]. According to Kuznik et al. [16], the name differential scanning calorimetry is very clear:

Calorimetry: The measurement of the quantity of heat absorbed or released by a sample subjected to temperature change.
Differential: The above measurements on sample are done with respect to reference sample with known properties
Scanning: The thermal excitation with a linear temperature ramp



Fig. 23. Hermetic aluminum sample pan and lid set.

5.1.2. *Analysis protocol*

The analysis procedure in pictorial form is shown in Fig. 22 and is explained herein.

5.1.2.1. Calibration. The purpose of calibration is to minimize any measurement uncertainty by ensuring the accuracy of the instrument [93]. For DSC, heat flow and temperature calibrations should be done periodically [90]. Typically indium is used as a calibrating material. In order to obtain accurate results, baseline slope and offset calibrations require heating an empty pan through expected temperature range in the experiment [90]. Calibration program is then used to flatten the baseline and zero the heat flow signal. It needs to be pointed out here that the type of purge gas and flow rate affects calibration. Therefore, nitrogen, which is inert, economical, least affected by changes in flow rate due to its low thermal conductivity and provide good sensitivity is preferred [91]. Additionally, it removes moisture (if any) and oxygen from the cell that may have accumulated over time [94]. It is worthy to mention here that too slow flow rate may cause moisture accumulation and early aging of the cell while too fast flow rate may cause excessive noise. For nitrogen, the preferred flow rate is 50 mL/min [90,91].



Fig. 24. Sample encapsulating press used to hermetically seal sample pan [94].

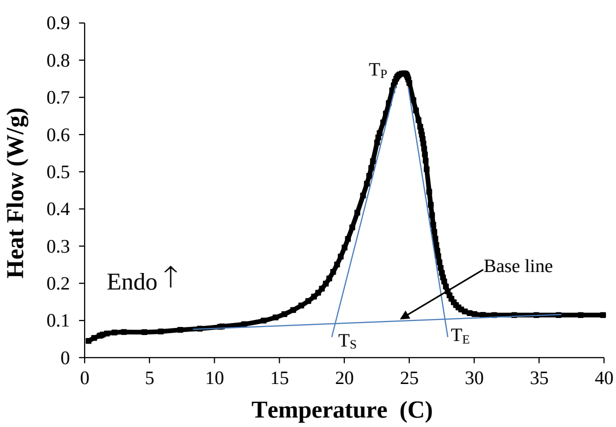


Fig. 25. DSC curve.

5.1.2.2. Sample preparation. Sample preparation includes selecting the appropriate weight and size of the sample, selecting the pan type and material and encapsulating the sample pan [90].

5.1.2.2.1. Sample weight and size. Larger samples will increase sensitivity but it will decrease the resolution. Therefore, the goal is to have heat flow rate in transition of interest in between 0.1 and 10 mW. Normally, the sample weight is in between 5 and 20 mg [90].

As far as the sample size is concerned, it should be made as thin as possible and for reproducibility it should be ensured that a good contact is maintained between the sample and the bottom of the pan. For powdered samples, it should be distributed uniformly

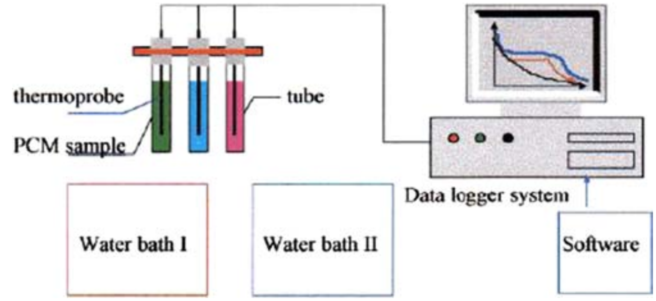


Fig. 26. A schematic diagram of the experimental rig [16].

across the bottom of the pan. This will minimize the thermal gradient [90].

5.1.2.2.2. Sample pan materials and configuration. The selection of pan material and its configuration depends on a number of factors such as temperature range experienced during the experiment and reactivity of the sample with the sample pan material. In most cases, aluminum pans can be used in the temperature range −180 to 600 °C. However, if the sample has the ability to react with aluminum than platinum, copper or gold pans can be opted [90].

As far as the sample pan configuration is concerned, the pan can be hermatic, nor-hermatic or open [90]. However, hermatic pan (Fig. 23) is preferred due to obvious advantages such as better thermal contact, reduced thermal gradient in the sample, higher internal pressure resistance due to air tight seal and preservation of sample for further study [90]. In addition, when contact with cell atmosphere or the reaction of the sample gas is required, hermatic pan can be used by making a pin hole in the lid before sealing.

After deciding the sample pan material and configuration and keeping the sample in the sample pan, both the hermatic and non-hermatic pan should be sealed with the sample encapsulating press (Fig. 24). The sample and reference pan are then loaded into the DSC cell.

5.1.2.3. DSC cell. Two types of DSC cells are available i.e. heat flux and power compensating. In heat flux DSC, the sample and reference pans sit on the same thermoelectric disc [16,90], which transfers the heat to these pans [95]. The heat capacity of the sample will cause a temperature difference between the sample and reference pans [89,96]. This temperature difference leads to voltage difference which after making adjustments for thermocouple response is proportional to heat flow [95,96].

$$q = \Delta T/R = \Delta U/R{*}S \tag{1}$$

q=Heat flow, ΔT=Temperature difference between sample and reference, R=Thermal resistance of thermoelectric disc, ΔU= Voltage difference between sample and reference, S=Thermocouple response

In power compensated DSC, the sample and reference pans are placed on two independent heaters. The current is supplied to the two heaters and the difference in the power required to maintain the sample and the reference pan at the same temperature is used to calculate heat flow.

5.1.2.4. DSC curve and thermal properties. The thermal properties such as phase change temperature and thermal energy stored in unit weight can be determined by using commercially available softwares such as TA Universal Analysis 2000 [97]. The typical DSC plot is shown in Fig. 25. The phase change temperature is divided into starting, peak and ending temperatures. The starting and ending temperatures are the temperatures at the intersection of extrapolated baseline and the tangents to the DSC curve drawn at

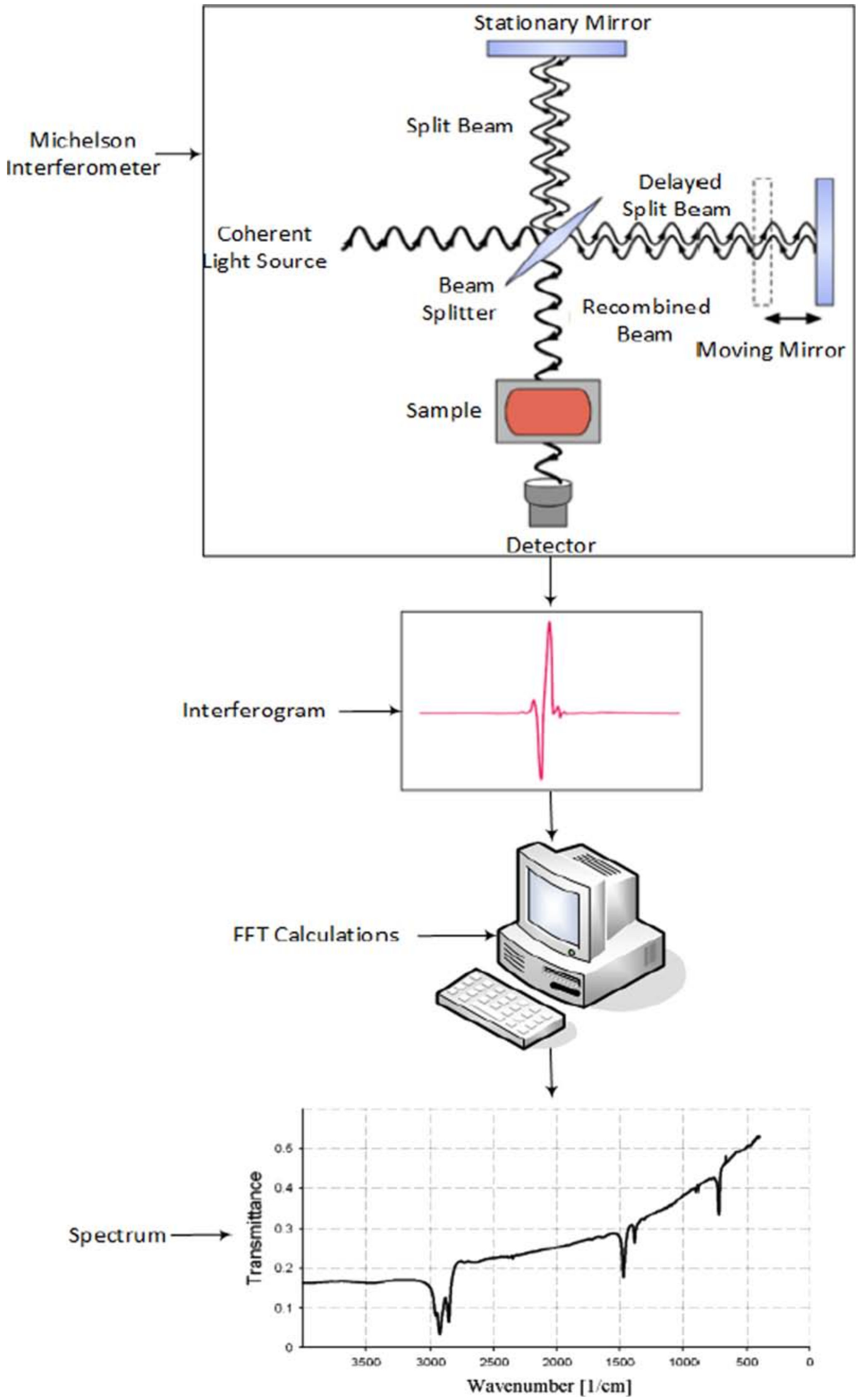


Fig. 27. FT-IR Analysis protocol {Michelson Interferometer from reference [105]}.

the inflection points to the left and right side of the peak while the peak temperature is the temperature at the peak point of DSC curve. The thermal heat stored in the unit weight of PCM is obtained by dividing the integrated area between the baseline and the DSC curve with a temperature rising rate in the DSC test. This value is calculated automatically by the software [54]. It is worthy



Fig. 28. Perkin-Elmer spectrometer model no. PE-100.



Fig. 29. The Specac Manual Hydraulic Presses [106].

to mention here that the user can choose different types of baselines such as linear, sigmoidal horizontal, sigmoidal tangent and extrapolated to calculate the thermal energy stored in the unit weight of PCM [94,97].

5.1.2.5. Differential thermal analysis (DTA). Differential Thermal Analysis, a thermoanalytic technique, appears to have been first employed by Le Chatelier in 1887 [98]. In DTA, the heat supplied to the sample and the inert reference remains the same while measuring the temperature and temperature differences (between the sample and the reference) associated with material changes as a function of time and temperature in a controlled atmosphere [11]. The plot of differential temperature versus temperature or time is known as a DTA curve.

5.2. T-history method

For the testing of large samples, Zhang and Jiang [25] proposed T-history method. This method allows the simultaneous determination of thermophysical properties of numerous PCMs (Fig. 26). The thermophysical properties are extracted from the temperature versus time curves of the PCM and comparing the curve with the temperature versus time curve of the reference material (usually pure water) [16]. With this method, the authors measured the thermophysical properties of numerous PCMs and found that the results are in agreement with those reported in literature. This method was improved by Marin et al., Hong et al. and Peck et al. [99–101]. For experimental details, the readers are referred to [25].

6. Chemical compatibility analysis-Fourier transform infrared spectroscopy (FT-IR)

6.1. Introduction

For PCM based building applications, FT-IR has been successfully used to determine the chemical compatibility between the components of composite PCM i.e. the PCM and the container/supporting material/encapsulation. With the invention of world's first commercial FT-IR spectrometer (Model FTS-14) in 1969 [102], FT-IR became the preferred method of spectral analysis. The term FT-IR originates from the fact that it uses Fourier transform, a diverse and versatile analytical technique, to convert the raw data into actual spectrum. Since the infrared spectrum represents the finger print of a sample [103] therefore it can be positively used for qualitative analysis. The major advantage of FT-IR includes high speed (Flegett advantage), improved sensitivity (Jacquinot advantage), mechanical simplicity and self-calibration (Connes advantage) [104].

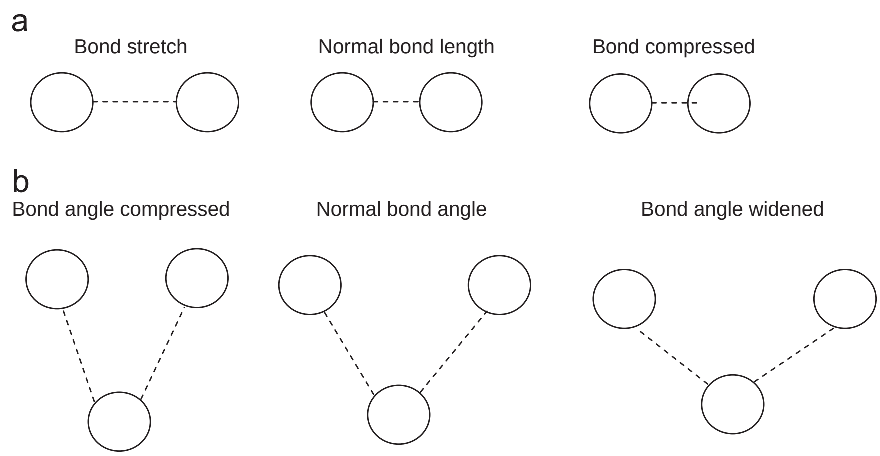


Fig. 30. Molecules (a) Stretching and (b) Bending [107].

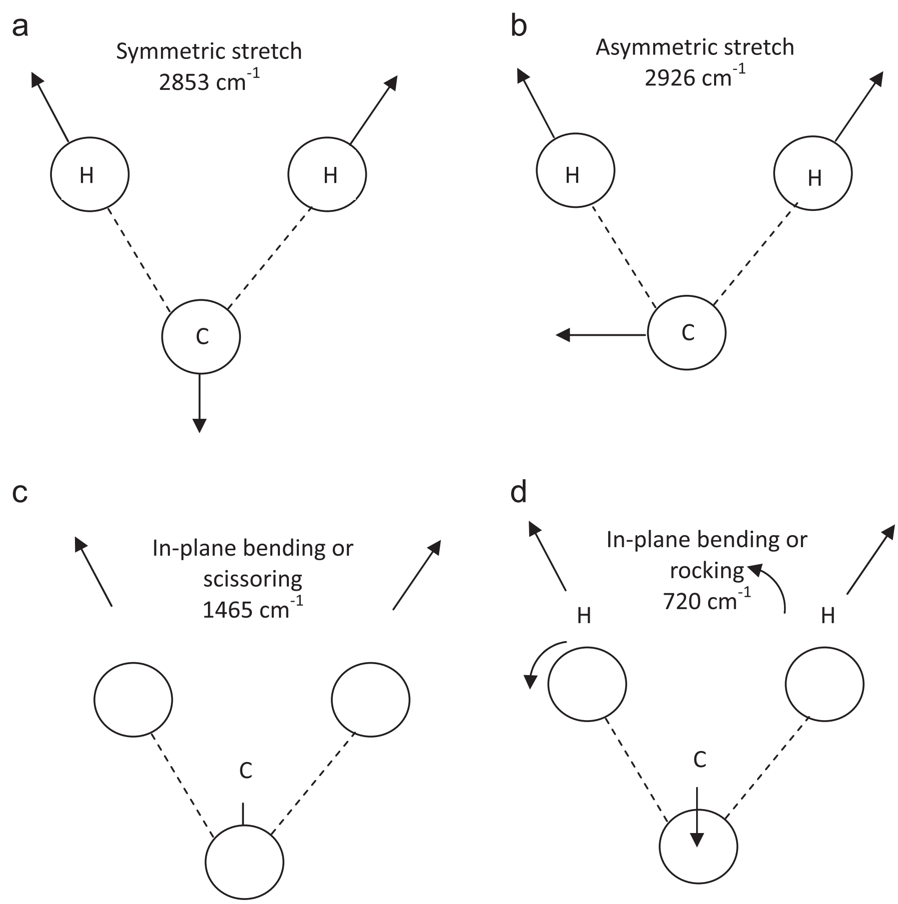


Fig. 31. Molecules (a) Symmetric Stretch (b) Asymmetric stretch (c) Scissoring (d) Rocking [107].

6.2. Fourier transform infrared spectroscopy analysis protocol

The FT-IR analysis procedure (Fig. 27) that is applicable to composite PCM in powder form, for example, PCM contained in perlite, graphite, silica fume, vermiculite, kaolin, etc. is described. The Perkin-Elmer spectrometer model no. PE-100 is shown in Fig. 28.

6.2.1. Sample preparation

The powdered sample and the KBr are usually heated in oven for 24 h at 105 °C followed by mixing in 1:100 (powder:KBr) ratio in controlled humidity environment. In order to ensure that the powder is randomly oriented, KBr pellets are prepared. For this, the mixed sample is usually pressed at 10 tonnes for 1 min in any hydraulic press (The Specac 15 tonnes Manual Hydraulic Presses Fig. 29). The obtained KBr pellet is then placed in the sample compartment and infrared spectrum, in transmittance or any other mode, is obtained via Spectrum Analysis software. It is noteworthy to mention here that in order to remove the instrumental characteristics from the spectrum, a background spectrum must be measured. This is done by taking the reading with no sample in the sample compartment.

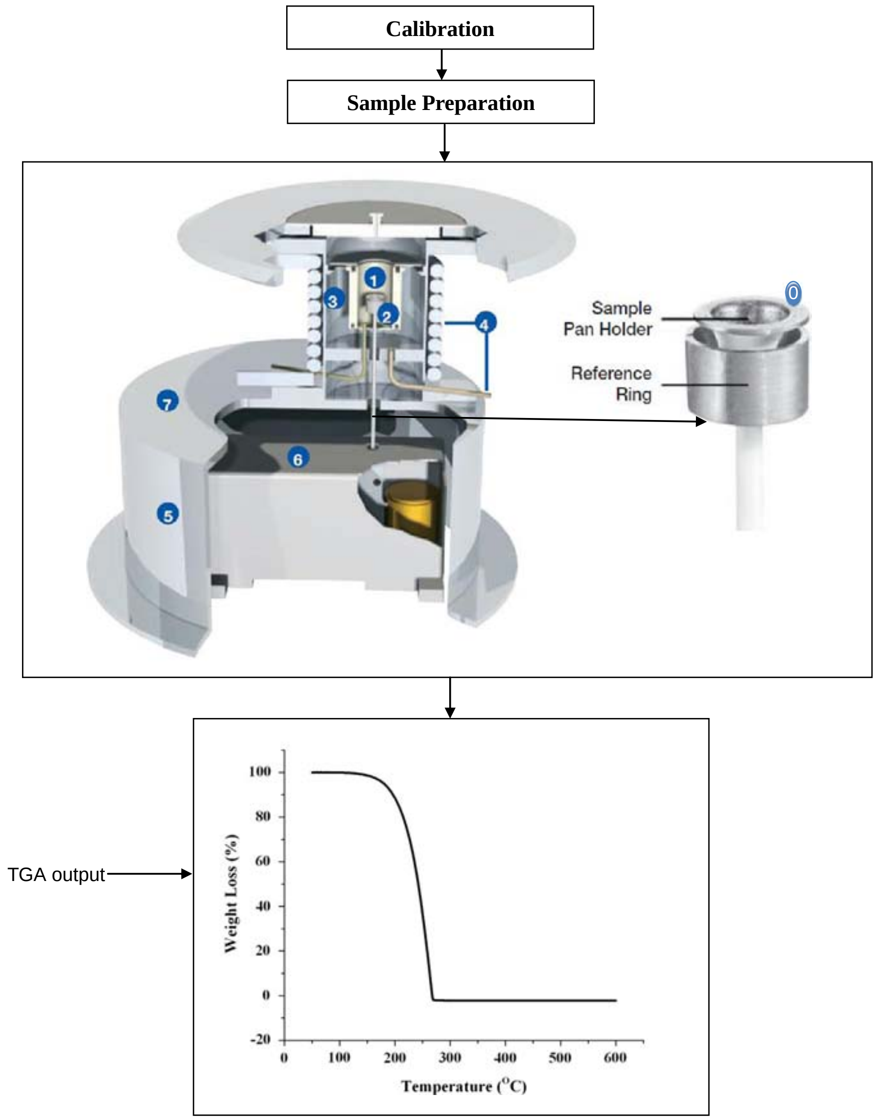


Fig. 32. TGA analysis protocol {TGA apparatus from reference [111]}.

6.2.2. Michelson interferometer

It has the following components.

6.2.2.1. Infrared source. Infrared energy emitted from a polychromatic infrared source is directed towards the beam splitter.

6.2.2.2. Beam splitter. It is an optical device which divides the beam into two. Fifty percent of the light from the beam splitter is refracted towards the fixed mirror while the other 50% is transmitted towards the moving mirror. The reflected light from these mirrors is collected back by the beam splitter and 50% of it is passed to the sample.

6.2.2.3. Sample. Depending upon the type of analysis, the beam entering the sample chamber is transmitted through or reflected off the surface of sample. Here, the wavelength of IR that has the same natural frequency as the molecules constituting the sample are absorbed. Since the final spectrum is created by the molecular vibration therefore it is also known as the molecular vibration spectrum.

6.2.2.4. Detector. The beam from the sample is passed to the detector which yield interferogram signal.

6.2.3. Computer/FFT calculations and FT-IR spectrum

The measured interferogram is converted into spectrum through computer via a mathematical technique known as Fourier Transformation. The desired spectral information is then available to the analyst. Based on the experience of the analyst, he/she can attempt to assign the bands obtained from the infrared spectrum by comparing it with the correlation tables, which is a catalog of published groups and their characteristics absorption frequencies.

6.3. Types of molecular vibrations in FT-IR

The atoms in the molecule are continuously vibrating causing change in the bond lengths and angles. A molecule absorbs infrared energy when its natural frequency coincides with the frequency of incident infrared light. The motion of molecules can be described by two types of vibration i.e. stretching and bending [107] (Fig. 30). In stretching vibration, the atoms move along a line so that the distance between them either increases or decreases. In other words, stretching vibration produce a change in bond length.

Also, stretching vibration can have variation i.e. it can be symmetrical or anti-symmetrical. In bending vibration, a bend produce change in the bond angle and bending of the molecule can be in plane or out of the plane. It can also have variation i.e. scissoring, like the blades of a pair of scissors or rocking, where the atoms move in the same direction.

The different types of vibration of molecules are demonstrated by taking into account CH_2 group in hydrocarbon (Fig. 31). It can be seen that stretching vibration is observed at higher wavenumber than bending vibration. Since wavenumbers are directly proportional to energy therefore stretching vibration require more energy than bending ones. Similarly, asymmetric stretch requires more energy than the symmetric stretch.

7. Thermal stability analysis-thermogravimetric analysis (TGA)

7.1. Introduction

For PCM based applications, thermal gravimetric analyzer has been used to determine the thermal stability of the composite PCM. It is an experimental method of thermal analysis in which the change in weight of a material is observed as a function of temperature or time while the material is subjected to a controlled temperature program in a controlled environment [108,109]. Several researchers have used this technique to ensure that the composite PCM is stable in the working temperature range [57,86]. Also, it is used to ensure that the components of composite PCM are decomposing separately.

7.2. TGA analysis protocol

The step by step TGA analysis procedure described herein is graphically shown in Fig. 32.

7.2.1. Calibration

For TGA usually the following calibrations are done.

Weight calibration

Temperature calibration

Heat flow calibration

Weight calibration is usually performed at the installation of the instrument. However, it should also be performed when the instrument is moved or when the results deviate from those expected [109,110].

The purpose of temperature and heat flow calibration is to synchronize the sensor and furnace to the known melting and heat flow properties of reference materials. Indium having melting temperature of 156.6 °C and heat of fusion of 28.45 J/g is usually used to verify the temperature and heat flow calibrations. It is suggested that baseline correction should be performed before the temperature and heat flow calibration [110]. Also, nitrogen which is inert and least affected by changes in the flow rate is usually used as purge gas [109]. It is also worth mentioning here that some instruments use curie point transition method for temperature calibration. For this method, nickel is the most commonly used curie point reference material [109].

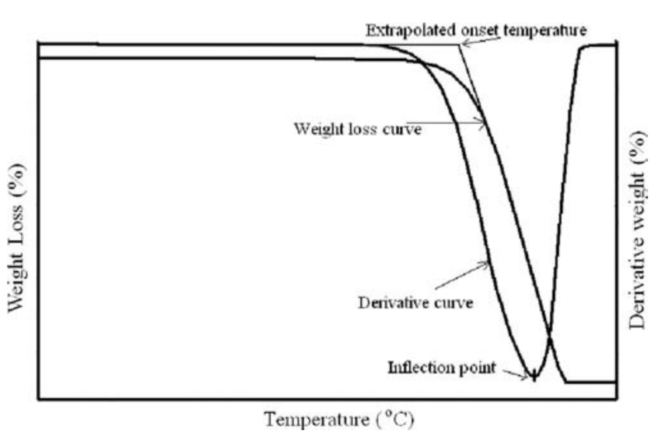


Fig. 33. TGA curve showing extrapolated onset temperature and inflection point.

7.2.2. Sample preparation

In order to ensure reproducibility it is suggested that same sample weight should be used and it should be tried to cover the bottom of the pan with the sample material. Also, instead of using one large chunk it is preferred to use many small pieces since it will expose a large surface area of the sample purge [109]. For most applications, the weight of the sample should be in between 2 and 50 mg.

As far as the sample pan material is concerned, ceramic and platinum pans are available and they are capable of accommodating liquids, powders, solids, films, etc. [109].

7.2.3. TGA apparatus

TGA depends on a high degree of accuracy in mass and temperature measurements. Therefore, the basic instrumental requirements for TGA are a precision balance and a programmable furnace that is heated or cooled during the entire experiment [108,109]. For better understanding, the working of the main components of STA 6000 is briefly outlined [111].

The STA 6000 consists of a sample pan holder that is supported by a precision balance through sensor (0 and 2).

The sample pan holder resides in the furnace which enables accurate heating and cooling during the experiment (1).

The corrosion resistant alumina furnace allows for a wide variety of reactive gases (3) to be used during the experiment.

For rapid cooling of the furnace, the apparatus is integrated with chiller and forced air cooling system (4). This also ensures more sample process in less time.

The stainless steel walls thermally isolate the balance from the furnace (5).

The constant environment for the balance is maintained by the use of balance purge gas. It also protects the balance from material evolving from the sample as well as reactive sample purge gas (6).

The sample environment is controlled by the sample purge gas through mass flow controller (7) and depending on the type of analysis the purge can be inert or reactive.

It is worthy to mention here that the TGA apparatus is controlled by Pyris software [111].

7.2.4. TGA results

The results obtained from TGA can be presented as [108],

Thermogravimetric curve i.e. Weight versus temperature or time curve

Differential temperature curve i.e. Rate of loss of weight versus temperature curve

From thermogravimetric curve, we can determine the weight loss and extrapolated onset temperature which represents the temperature at which weight loss begins [109] while from differential temperature curve; we can determine the inflection point i.e. the peak of the first derivative (Fig. 33). This point represents the point of the greatest rate of change of the weight loss curve [109].

8. Measurement of thermal conductivity of PCM/composite PCM

In order to improve the performance of PCM in terms of heat transfer, it is necessary to determine the thermal conductivity of the PCM/composite PCM. The thermal conductivity of a sample

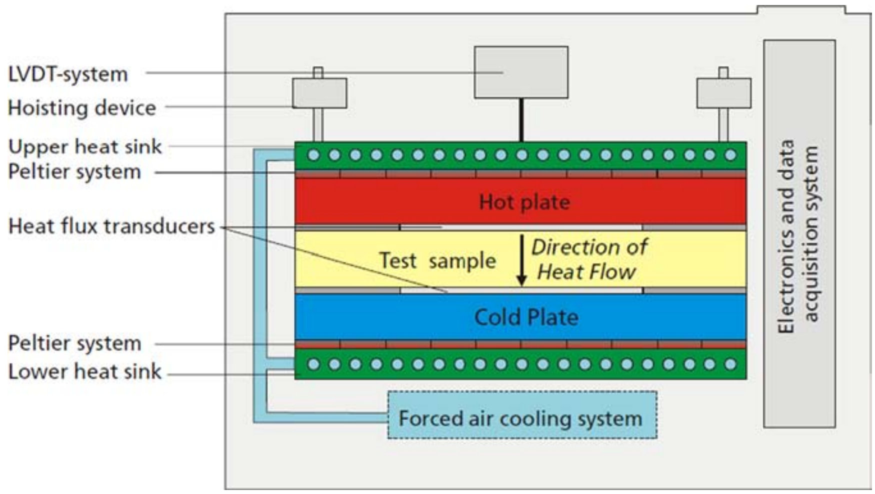


Fig. 34. Heat flow meter [114].

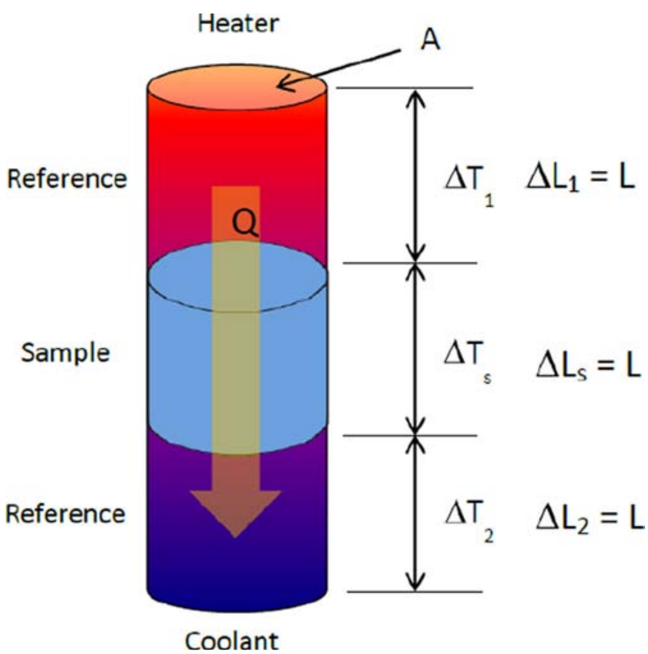


Fig. 35. Comparative cut bar method [116].

can be measured by steady-state and non-steady steady methods. In the steady state method, the measurements are made when the temperature of the material does not vary with time, i.e. at constant signal. Therefore, the signal analysis is simple and straightforward [112]. In non-steady state method, the measurement are made during the process of heating up i.e. the signal is studied as a function of time. It can be performed more quickly however; in general, the mathematical analysis of the data is more difficult [112].

8.1. Steady state methods

Various methods are used to determine the thermal conductivity of samples under steady state condition. Some of them are briefly described here.

8.1.1. Heat flow meter method

This method is simple in concept, quick and appropriate for a wide range of test specimens such as solid or loose-fill materials. It is applicable to materials having low thermal conductivity for example building insulations in the range 0.005 to 0.5 W/(m.K) and provide highly accurate results provided it has been calibrated properly [113]. In this method, the test sample is placed between two parallel plates set at different temperatures (Fig. 34). The heat flow through the sample is measured by a (calibrated) heat flux transducer. The test is completed once thermal equilibrium is reached. The thermal conductivity of the sample is calculated using Fourier′s law of heat conduction by the following formula

$$k = N*(V*\Delta x/\Delta T) \tag{2}$$

where $k=$ thermal conductivity of the sample, $N=$ the calibration factor that relates the voltage signal of the heat flow transducer to the heat flux through the sample, $V=$Voltage signal of the heat flow transducer, $\Delta x=$ thickness of the sample, $\Delta T=$ temperature difference across the sample.

8.1.2. Cut bar or flat slab comparative method

This method is most widely used for axial thermal conductivity testing and is especially useful for engineering materials including ceramics, polymers, metals and alloys, refractories, carbon, graphite, etc. It is applicable to materials having effective thermal conductivities in the range 0.2–200 W/(m.K) over the temperature range between 90 and 1300 K [115]. In this method, the test sample under load is sandwiched between the reference samples with known thermal properties (Fig. 35). Heat is then supplied through the top and made to move downward. At equilibrium conditions, the thermal conductivity is derived by comparing the thermal gradient of the test sample and the reference samples. For comparative cut bar method, the thermal conductivity of the unknown sample can be derived from the following formula [116].

$$Q/A = k*(\Delta T_S/L) = k_R*(\Delta T_1 + \Delta T_2)/2*(1/L) \tag{3}$$

where, $Q=$ amount of heat passing through cross sectional area A, $A=$ cross sectional area, $k=$ Thermal conductivity of the sample, $k_R=$ Thermal conductivity of the reference, $\Delta T_1=$ Temperature difference over a distance of ΔL_1, $\Delta T_2=$ Temperature difference over a distance of ΔL_2, $\Delta T_S=$ Temperature difference over a distance of ΔL_S.

It is worthy to mention here that when the test sample and the reference samples are right-circular cylinders of equal diameter the technique is known as cut bar method while the technique is called the flat slab comparative method when the cross sectional dimensions are larger than the thickness [115]. It also needs to be pointed out here that in this test method, the heat losses are minimized by using longitudinal guard.

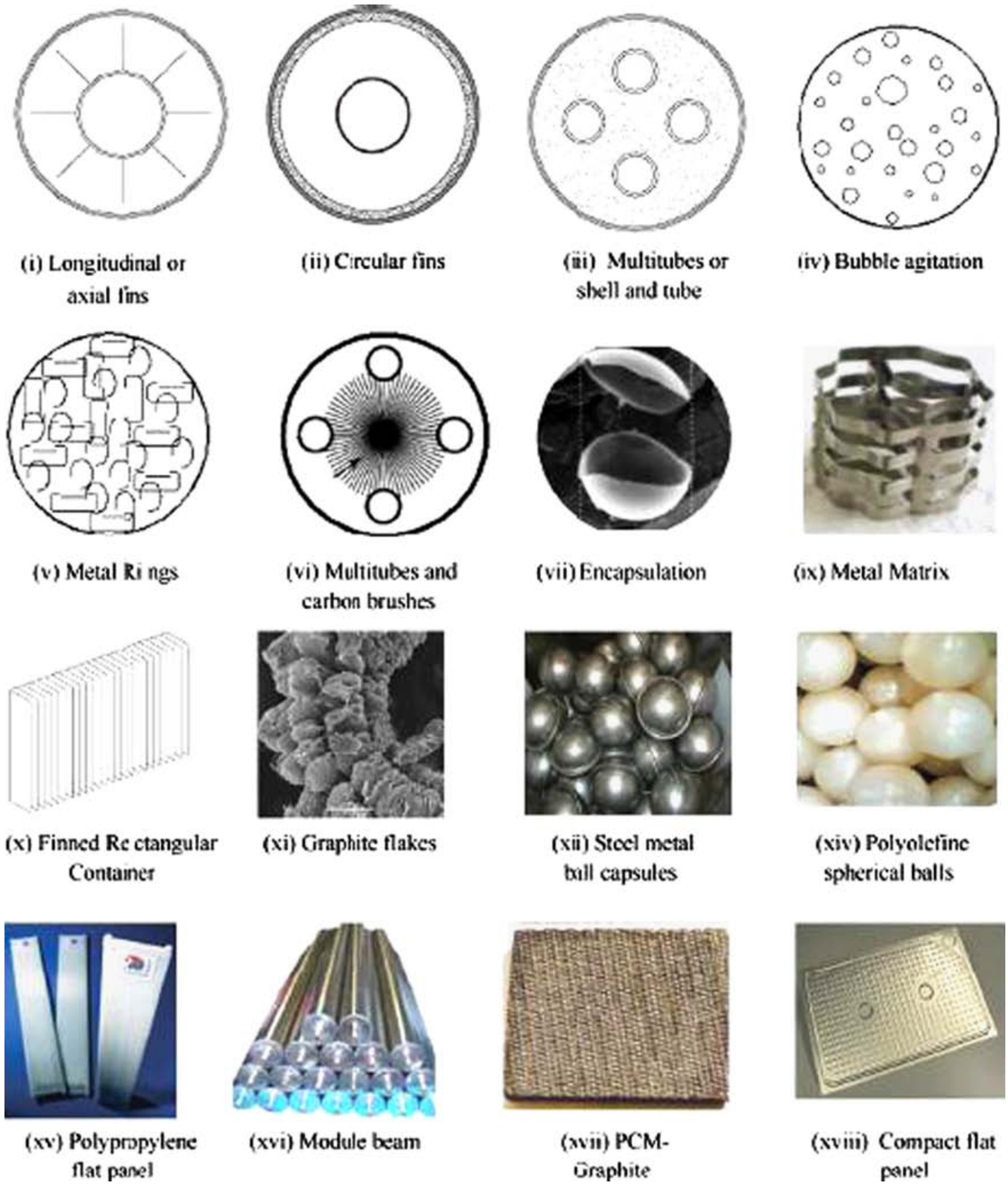


Fig. 36. Heat transfer enhancement methods employed in PCM research.

8.2. Non-steady state methods

In literature, the hot wire method has been generally used to determine the thermal conductivity of composite PCM [117,118].

8.2.1. Hot wire method

This method is used to determine the thermal conductivity of refractory brick, ramming mixes, powdered materials, granular materials, etc. It is usually applicable to isotropic materials having thermal conductivities less than 15 W/(m.K) over the temperature range between room temperature and 1500 °C [119]. In this method, a constant electric current is applied to pure platinum wire which is placed in between the sample. The rate at which the wire is heated is dependent upon how rapidly the heat flows from the wire into the sample which is held at constant temperature. The rate of temperature increase of wire is measured by its increase in resistance. Thermal conductivity is determined by applying Fourier equation [119].

Frusteri et al. [118] and Sari et al. [117] determined thermal conductivity of composite PCM using the hot-wire method. Using

Table 9
Thermal characteristics of various gypsum-PCM combinations [29].

PCM	Melting point (°C)	Freezing point (°C)	Average latent heat of impregnated gypsum (J/g)
Capric-lauric acid	17	21	28
Butyl stearate	18	21	30
Propyl palmitate	19	16	40
Dodecanol	20	21	47

Carslaw and Jaeger theory, they determined the thermal conductivity by the following formula.

$$k = (U*I/4\Pi L)/(\Delta T/\Delta(\ln t)) \quad (4)$$

where k=thermal conductivity of the sample, U= applied voltage, I= current circulating along the platinum wire, L= length of the platinum wire, ΔT= temperature change, $\Delta(\ln t)$= logarithmic time interval for the associated time t_2 and t_1.

9. Thermal conductivity enhancement of PCM

One major issue that requires attention is that most of the PCMs have low thermal conductivity [120]. Several techniques have been used to improve the thermal conductivity of the conventional PCMs [10,36] for instance (a) impregnation of high conductivity porous material (copper and aluminum matrices, graphite) with the PCM; (b) dispersing highly conductive particles (graphite, copper, aluminum, silver) in the PCM; (c) placing metal structures (lesser rings, metal beads, metal fins) in PCM (d) using low density highly conductive materials (carbon fibers) in PCM; (e) microencapsulating PCM (steel balls) to improve heat transfer surface. This shows that thermal conductivity of PCM can be improved by incorporating materials having high thermal conductivity. However, the addition of these materials may lead to decrease in the storage capacity of pure PCM. Hence, it is necessary to determine the optimum mass/volume fraction of such additives which would result in a substantial increase in thermal conductivity of PCM without affecting much the storage capacity of pure PCM. Some of the common techniques used to enhance the thermal conductivity of the PCM are shown in Fig. 36. The in depth literature on this topic can be found in references [10,36,43,121].

10. Building applications for phase change materials

During the last two decades, integration of PCM in wallboards and concrete has regained interest. Therefore, in this section we focus on experimental investigations carried out on PCM enhanced wallboard and concrete for building applications.

10.1. PCM enhanced wallboards

Wallboard is considered suitable for incorporation of PCM because of the following reasons [29].



Fig. 37. 60 wt% paraffin microencapsulated in 5 cm thick copolymer composite wallboard [127].

(a) They are economical and commonly used in lightweight construction.
(b) They have larger heat exchange area and smaller heat exchange depth.
(c) PCM is held by them under surface tension forces.
(d) Existing facilities can be used for the production.
(e) Ease of testing.

However, as pointed out by various researchers [10,12], the efficiency of PCM wallboards will depend on various factors such as (a) the PCM selected and its phase transition temperature, (b) the manufacturing technique, (c) the latent heat capacity per unit area of the wall, (d) the orientation of the wall, (e) climate conditions, (f) direct solar gains, (g) ventilation rate and (h) color of the surface. Some of the prominent works by various researchers are described herein.

The performance of gypsum wallboards impregnated with PCMs (Capric-lauric acid, Butyl stearate, propyl palmitate, dodecanol) was investigated by Hawes et al. [29]. They used direct incorporation and immersion techniques and successfully impregnated 25–30 wt% PCM in gypsum wallboards (Table 9). In comparison to conventional wallboards it was found that PCM wallboards have

(a) Eleven-fold increase in energy-storage capacity through a 4 °C rise.
(b) Comparable flexural strength.
(c) Depending upon the type and content of PCM, thermal conductivity values were within the range of ± 15%.
(d) Excellent fire resistance and slightly greater flame travel than for the conventional board.
(e) Good compatibility with paints and wallpapers.
(f) More durable in moist environment.
(g) Twenty-two percent increased weight than conventional wallboard but still within the weight limits accepted by the industry.

The same team conducted full scale thermal testing of rooms (2.29 × 2.27 × 2.45 m) with gypsum wallboards [123]. On average, 25.2 wt% of PCM (Emerest 2326) was impregnated in gypsum wallboard through immersion technique. It was concluded that PCM wallboard may be considered a suitable candidate for thermal energy storage application. The volatile organic compound concentration levels in both the rooms (with and without PCM) were almost similar and within acceptable limits by ASHRAE standard. Furthermore, the unpleasant odor in rooms with PCM wallboard could be completely removed if the PCM wallboards are kept at 93 °C for several hours [40].

Shilei et al. [124] experimentally evaluated the performance of gypsum wallboards impregnated with 26 wt% PCM (mixture of capric and lauric acid) in Shenyang located in northeast China in winter. The thermal performance of rooms (5 m × 3.3 m × 2.8 m) with and without PCM gypsum wallboards was monitored for three consecutive days. For the tested periods, the rooms were heated by 2040 W electric heating membrane installed in the ceiling. According to the test results, the maximum temperature fluctuation in PCM wall room was 1.15 °C lower than ordinary wall room. Furthermore, the thermal flow in the PCM wall room was lower than ordinary wall room. Thus, PCM wallboards can reduce the indoor temperature fluctuations and the scale of heating equipment as well as the related investment cost.

In order to investigate light building envelope, an experimental investigation was carried out with copolymer composite wallboard microencapsulated with 60% paraffin (Fig. 37) [125]. The test cell was totally controlled and three cases were evaluated namely a summer day, a winter day and a mid-season day. From the test

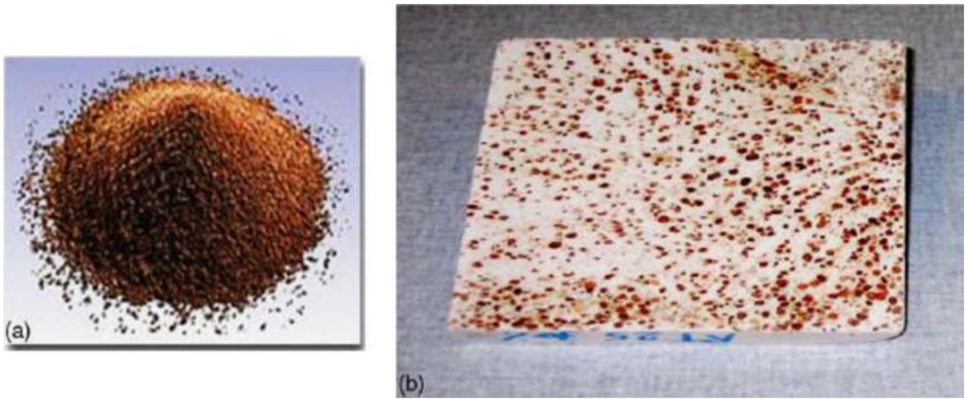


Fig. 38. (a) Granulates filled with paraffin (b) gypsum-granulate sample [131].



Fig. 39. View of the test cell [132].

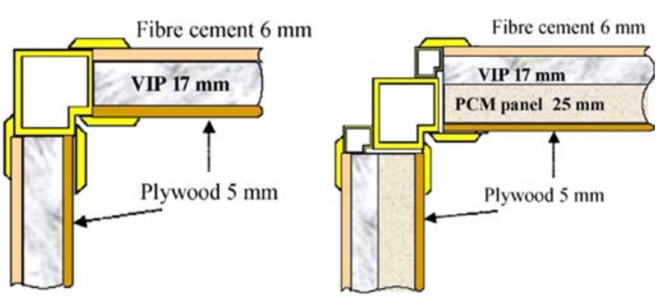


Fig. 40. Cross-section of the wallboards of the test-cell (a) without PCM (b) with PCM [132].

results it was found that with PCM wallboard, the air temperature and wall surface temperature fluctuations are reduced. The air temperature in the room with PCM reduced up to 4.2 °C. In addition, the room with PCM avoided uncomfortable thermal stratifications. Furthermore, the PCM copolymer composite wallboard was used in a room (5.2 m × 3.55 m × 2.7 m) of renovated office building and the test results were monitored for 1 year. It was shown that the PCM wallboards enhanced the thermal comfort of residents due to air temperature and radiative effects of the walls [126].

The thermal performance of the PCM gypsum wallboard was examined by Neeper [128]. The three parameters evaluated were

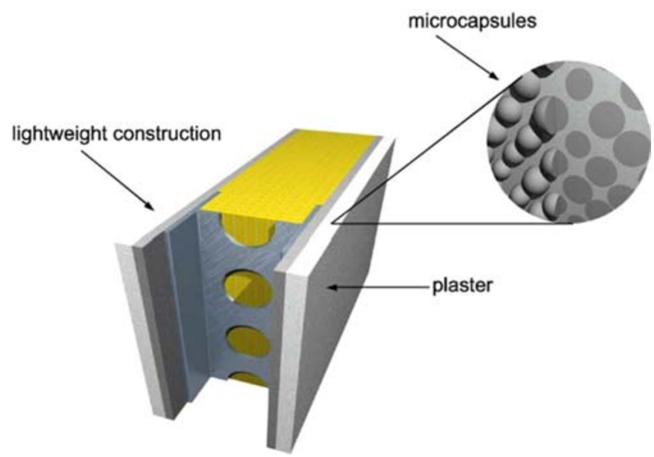


Fig. 41. Schematic view of lightweight wall with PCM microcapsules integrated into the interior plaster [42].

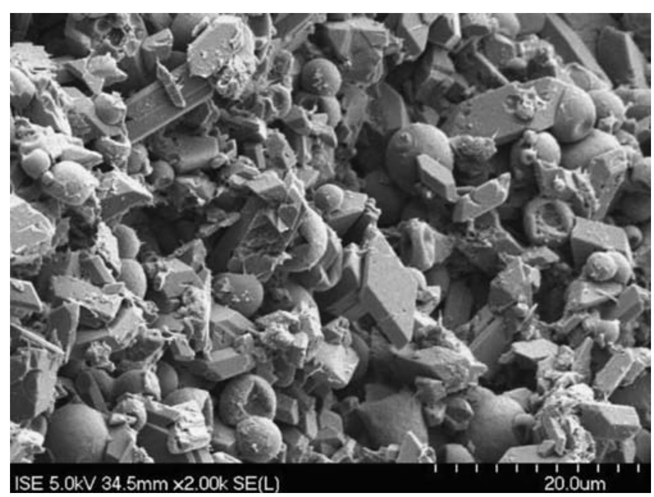


Fig. 42. SEM of PCM microcapsules in gypsum plaster [42].

(a) the melting temperature of the PCM (b) the temperature range over which the melt occur and (c) the latent capacity per unit area of wallboard. It was found that the diurnal storage achieved in practice may be limited to the range 300–400 KJ/m^2. Moreover, the maximum diurnal energy storage occurs when the PCM melt temperature equals the average wallboard temperature.

Athienitis et al. [129] carried out experimental and numerical simulation study on full scale outdoor test room (2.82 m × 2.22 m × 2.24 m) with PCM gypsum wallboard. Butyl stearate was incorporated in gypsum wallboards by 25 wt%. An explicit



Fig. 43. Two office buildings equipped with PCM plaster [42].

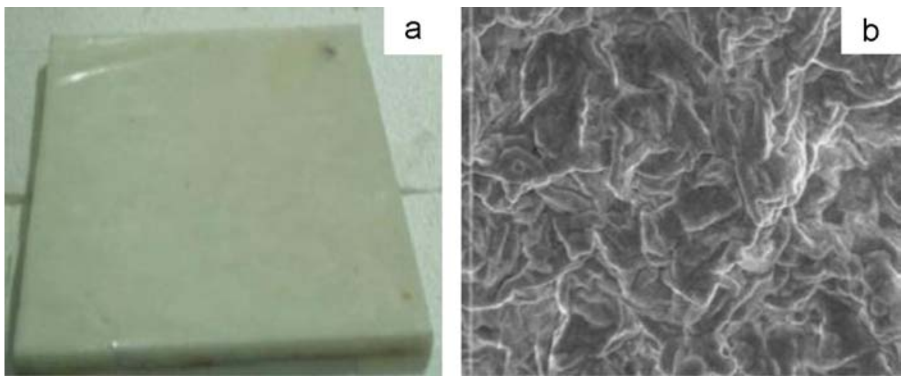


Fig. 44. (a) Photo of shape-stabilized PCM plate (b) SEM of shape-stabilized PCM [44].

finite difference model was developed to simulate the transient heat transfer process in the walls. According to the test results, the gypsum wall boards may reduce the maximum temperature by 4 °C during the daytime and can significantly reduce the heating load at night.

The thermal performance of gypsum boards containing 37.5 and 47.5% percentage by weight of PCM was evaluated by Oliver [130]. Several parameters (air temperature and velocity as well as thickness and location of board) were analyzed to study the influence of the boundary conditions on the energy exchange. In addition, several construction materials (gypsum board, brick wall, thermal brick wall and sandwich panel made with aluminum sheets with insulation core) were tested. It was found that 1.5 cm thick gypsum board with PCM stores five times the thermal energy of a laminated gypsum board. Furthermore, it has the same energy as a 12 cm thick brick wall within the comfort temperature range (20–30°C).

With the aim to build a light building envelope, Ahmad et al. [131] investigated three different types of PCM wallboards: (a) a polycarbonate panel filled with paraffin granulates (Fig. 38) (b) a polycarbonate panel filled with polyethylene glycol PEG 600 and (c) a PVC panel filled with PEG 600 and coupled to a vacuum isolated panel. Test results showed that PVC panel filled with PEG 600 met authors′ requirements (light building envelope and having high heat capacity storage). In addition, the panel did not show any deterioration after 400 thermal cycles.

The thermal inertia of light envelopes, which are frequently being used in modern buildings, was improved by Ahmad et al. [132] by incorporating phase change material coupled with a vacuum insulation panels (VIP). Two test cells were designed and each consisted of one glazed face and five opaque faces insulated with VIPs (Fig. 39). The thermal inertia of one of the cell was increased by installing five PCM panels. The details of walls with and without PCM are shown in Fig. 40. During summer, the efficiency of PCM test cell was found to be remarkable with a reduction in temperature amplitude of 20 °C. In winter, the PCM cell helped to prevent negative indoor efficiently. Moreover, the PCM panels showed good thermal performance even after 480 thermal cycles.

Borreguero et al. [133] investigated the thermal performance of gypsum blocks (10 cm × 6 cm × 3 cm) incorporated with microencapsulated PCM (Rubitherm® RT27). The performance of three gypsum wallboards one without PCM and the other two with 4.7 and 7.5 wt% microencapsulated PCM was evaluated. It was found that the higher the amount of PCM incorporation in the gypsum wallboard, the lower or higher the external wall temperature for heating or cooling process respectively. Moreover, the incorporation of PCM microcapsules to the wall increased the time needed to reach the steady state. Thus, testifying the material insulation capacity through increased PCM content in the wall.

Sari et al. [134] prepared form-stable phase change wallboard by incorporating eutectic mixture of capric and stearic acid into gypsum wallboard. The gypsum wallboard absorbed 25 wt% PCM and did not show any sign of leakage even after 5000 cycles. The melting temperature and latent heat of form-stable phase change wallboard were found to be 24.68 °C and 48.32 J/g. The thermal performance test on small test room ($100 \times 100 \times 100\ mm^3$) showed that form-stable gypsum wallboard reduced the indoor center temperature by 1.3 °C. Moreover, large scale thermal performance testing was suggested by the authors.

Schossig et al. [42] investigated the thermal performance of lightweight buildings integrated with microencapsulated PCM (Figs. 41 and 42). Two different PCM products (dispersion based plaster with 40% weight PCM-6 mm thickness and gypsum plaster with 20% weight PCM-15 mm thickness) were tested each for a period of 1 year. Test results showed that microencapsulated PCM were effective in reducing the cooling demand and increased the comfort of lightweight buildings. During three weeks period, the

reference room was warmer than 28 °C for 50 h while the PCM room was only 5 h above 28 °C. According to the authors; micro-encapsulated PCM has the advantage of easy application, good heat transfer and no need for protection against destruction. However, for the successful application of PCM it is necessary that the stored energy can be discharged during the night with adequate ventilation. It is worth mentioning here that this product is in market and some office buildings have been equipped with them (Fig. 43).

The experimental and numerical study regarding the application of shape stabilized PCM in buildings was carried out by Zhang et al. [44]. The thermophysical properties of shape stabilized PCM (Fig. 44) developed by the authors are enlisted in Table 10. Paraffin was used as phase change material while HDPE or a composite was used as a supporting material. For the case of composite, each component had its role; HDPE endowed rigidity to PCM; SBS strongly absorbed the PCM while graphite or carbon fibers were used to enhance the thermal conductivity of the system. For the purpose of verifying the model, a cubicle having dimensions of 3 m × 2 m × 2 m was constructed in Tsinghua University, China (Fig. 45).

Following conclusions were drawn,

(a) The concentration of 80% paraffin in shape stabilized PCM was found to be optimum.
(b) The experimental and simulation results were in good agreement.
(c) From simulation results, it was found that optimal melting temperatures of shape stabilized PCM used in buildings located in Beijing and Shanghai were 20 and 25 °C respectively. This suggests that the optimal melting temperature of PCM varies with the climate conditions.
(d) For winter season in Beijing, the latent heat of fusion of 120 kJ/kg was suggested as optimal value.
(e) For studied cases, the thermal conductivity had a little effect on lowering the peak of indoor air temperature.
(f) The increase in air gap between the PCM plates and the floor covering was found to increase the indoor temperature swing. Therefore, it was suggested to eliminate the air gap as much as possible in practical applications Fig. 46.
(g) For practical application, the thickness of shape stabilized PCM layer should not exceed 20 mm.
(h) Tile or metal was suggested as floor covering materials.

The energy and environmental performance of a typical residential flat (Fig. 46) with PCM integrated in the external wall of living room and bedroom located in Hong Kong was evaluated by Chan [135]. The residential flat having an area of 95 m^2 was modeled by using building energy simulation program EnergyPlus developed by US-DOE. For simulation, split-type-air-conditioning units were operated during 1:00 pm to 10:00 pm in living room and from 11:00 pm to 7:00 am for bedrooms. Moreover, a typical weather data set representing the summer day was selected. It was found that the living room of a residential flat with west-facing integrated with PCM performed better in terms of decreasing the interior surface temperature up to a maximum of 4.14%. For the west facing case, an annual energy saving of 2.9% in air-conditioning system was achieved. However, keeping in view the average life span of residential building in Hong Kong (60 years), a long payback period of 91 years made the building integrated with PCM economically infeasible. In contrast, for environmental assessment, an energy payback period of 23.4 years was determined for west-facing case. Therefore, the energy saved can recover the embodied energy of the PCM wallboard and contribute to mitigation of greenhouse gases emission over the life span of the building

10.2. PCM enhanced cement mortar and concrete

Concrete is the most commonly used construction material with annual production of around 11 billion metric tonnes. "Man consumes no material except water in such tremendous quantities" [68]. The large thermal mass of the concrete walls can be advantageous especially in moderate climates where it can be used to store energy during the day and release it during night time therefore reducing the need for auxiliary cooling and heating [136]. Moreover, the energy storage capacity of concrete can further be enhanced by the incorporation of PCM into the concrete mixtures. Thermocrete, a PCM enhanced concrete, combines an appropriate PCM with a concrete matrix producing concrete with structural and thermostatic properties [12]. Concrete is considered suitable for incorporation of PCM because of the following reasons [32].

(a) They are most widely used construction materials.
(b) They can be formed into a variety of shapes and sizes.
(c) They have a larger heat exchange area and smaller heat exchange depth.
(d) Heat can be exchanged at faces and core surfaces and any combinations thereof.
(e) PCM is held by them under capillary and surface tension forces.
(f) Production and quality control can be easily achieved.
(g) Ease of testing.

In addition, Baetens et al. [12] with the help of example showed that PCM enhanced concrete has the overall heat capacity of 10 times more than gypsum wallboards. Some of the prominent works by various researchers are briefly described in this section.

The thermal performance of cement mortar prepared with *n*-octadecane/expanded graphite composite PCM was evaluated by Zhang et al. [65]. The percentage of *n*-octadecane/expanded graphite composite PCM in thermal energy storage cement mortar (TESCM) varied from 0.5 to 2.5 wt%. It was found that the compressive strength and thermal conductivity of TESCM decreased with the increase in the percentage of *n*-octadecane/expanded graphite composite PCM in TESCM. The maximum decrease in compressive strength and thermal conductivity values were 55 and 15.5% respectively. From thermal performance test on small test room of size 100 × 100 × 100 mm^3, it was found that TESCM containing *n*-octadecane/expanded graphite composite PCM is effective is decreasing the indoor center temperature and the decrease in the indoor center temperature is greatly enhanced with the increase in the percentage of *n*-octadecane/expanded graphite composite PCM in TESCM. It was concluded that TESCM containing *n*-octadecane/expanded graphite composite PCM are promising candidates for building applications.

The thermal performance of phase change materials in concrete was investigated by Hawes et al. [137]. The PCM investigated were butyl stearate, dodecanol, paraffin and tetradecanol while the concrete types used were autoclaved block, expanded shale block, ordinary Portland cement, pumice block and regular block. The study focused on the effect of concrete alkalinity, means of PCM incorporation and the effects of PCM and concrete temperature, immersion time and PCM dilution on PCM absorption during the impregnation process. It was shown that thermal storage can be increased up to about 300% and modifying the concrete by using pozzolans made it possible to use high alkaline concrete.

In another study, Hawes et al. [29] investigated the thermal performance of concrete blocks manufactured with different organic PCMs (butyl stearate, dodecanol, paraffin and tetradecanol). Direct incorporation and immersion techniques were used as a means of PCM incorporation and depending upon the type of concrete block used, up to 20% by weight of PCM was absorbed

Table 10
The thermophysical properties of the shape-stabilized PCMs [44].

1	Paraffin	Stryrene–butadiene–styrene	Paraffin/SBS/Wollastonite (70/25/5)	T_m=20.0 °C H_m=86.86 J/g
2	Paraffin	Stryrene–butadiene–styrene	Paraffin/SBS/Clay1 (70/25/5)	T_m=20.4 °C H_m=88.86 J/g
3	Paraffin	Stryrene–butadiene–styrene	Paraffin/SBS/Clay2 (70/25/5)	T_m=21.0 °C H_m=90.37 J/g
4	Paraffin	Stryrene–butadiene–styrene	Paraffin/SBS/Clay3 (70/25/5)	T_m=20.3 °C H_m=96.82 J/g
5	Paraffin	Stryrene–butadiene–styrene	Paraffin/SBS/$Mg(OH)_2$ (70/10/20)	T_m=20.6 °C H_m=82.97 J/g
6	Paraffin	Stryrene–butadiene–styrene	Paraffin/SBS/$Mg(OH)_2$ (70/10/10)	T_m=20.7 °C H_m=82.17 J/g
7	Paraffin	Stryrene–butadiene–styrene	Paraffin/SBS (70/30)	T_m=20.5 °C H_m=87.43 J/g



Fig. 45. Photo of experimental house, Tsinghua University, China [44].

(Table 11). It was found that the energy storage capacity of PCM concrete block is in the order of 200–230% of that of conventional block through a 6 °C change. In addition, in comparison to conventional blocks, PCM concrete blocks showed improved durability to freeze-thaw cycles, comparable flexural strength, reduced moisture absorptance and good fire resistance with minimal flame spread.

The macroscale investigation on the thermal performance of ordinary concrete blocks and those impregnated with PCM (Butyl Stearate and Paraffin) was investigated by Lee et al. [138]. The authors tested and compared two types of hollow core concrete blocks (20 × 20 × 40 cm^3) i.e. regular and autoclaved. The regular blocks were made with Portland cement steam cured at atmospheric pressure at 80 °C while the autoclaved blocks consisting of Portland cement and silica fume were steam cured at 180 °C under high pressure. The percentage of PCM absorbed by regular and autoclaved blocks was found to be 3.9 wt% and 5.6–8.6 wt% respectively. It was shown that the presence of PCM was found to double the heat storage capacity of the concrete block.

Hadjieva et al. [139] examined the heat storage capacity of autoclaved porous concrete after multiple thermal cycling. The cylindrical specimens (25.5 mm × 41.5 mm) were impregnated in sodium thiosulphate pentahydrate ($Na_2S_2O_3.5H_2O$) for 7 h at 75 °C. It was found that the PCM was absorbed by the pore and capillary spaces of porous concrete by up to 60 wt% and after repeated thermal cycling the absorption capacity reduced by 10%. The enthalpy of fusion of the PCM concrete was about 100 J/g. Thus, it was concluded that the autoclaved porous concrete is a good candidate as a supporting material and improves its structural stability during thermal cycling. It addition, it also eliminates the problems for example supercooling and phase segregation associated with the use of hydrated salts.

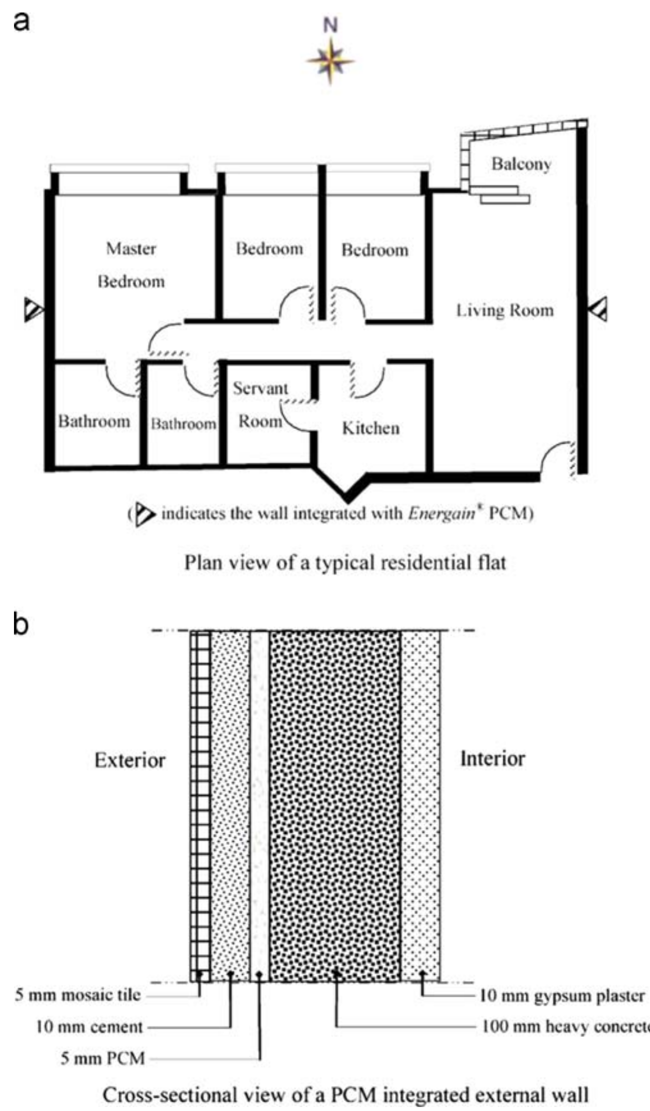


Fig. 46. Plan and cross-section of a typical residential flat, Hong Kong [135].

Zhang et al. [140] prepared thermal energy storage concrete by incorporating the PCM in porous aggregates. Thermal energy storage aggregates (expanded clay, normal clay and expanded shale aggregates) were prepared with vacuum impregnation technique. Test results showed that the maximum absorption of PCM by porous aggregates was 68 wt%. It was found that the aggregates with large pore connectivity factor and transport tunnel in boundary part can absorb more PCM. Furthermore, the

phase change behavior was affected by the volume fraction of PCM in concrete.

In another paper by the same authors [54], they utilized expanded fly ash, clay and perlite granular as supporting materials for organic PCMs. It was found that porous aggregates and PCM are chemically compatible, have large thermal energy storage density and are feasible for large scale processing. Moreover, among coating materials for porous aggregates, latex was found to be the best choice with sealing performance of 40-fold higher than that of normal cement paste and about seven-fold higher than that of the polymer modified cement paste.

Bentz and Turpin [136] experimentally investigated the effect of incorporation of PCM on temperature rise and decrease within 2 days of hydration of cement mortars at semi-adiabatic conditions. Three types of cement mortars were produced with water to cement ratio of 0.4. These mixes were (a) a control mix having no PCM produced with a non-porous coarse silica sand (b) a mix containing pre-impregnated expanded shale lightweight aggregate with 13.8% (by mass of dry LWA) paraffin wax as 100% replacement of sand and (c) a mix containing 100% paraffin wax particles (1 mm in size) as replacement of sand. According to the research findings, the use of PCM lowered the peak temperature by approximately 8 °C and delayed it by around 1 h. Therefore, the heat evolution in PCM-mortar was strongly influenced by the presence of PCM.

Table 11
Thermal characteristics of various concrete-PCM combinations [29].

Type of concrete	PCM	Melting point (°C)	Freezing point (°C)	Average latent heat of impregnated gypsum (J/g)	Age (days)
ABL	BS	15.2	19.3	5.7	692
REG	BS	15.4	20.4	5.5	391
PUM	BS	15.9	22.2	6.0	423
EXS	BS	14.9	18.3	5.5	475
ABL	DD	10.8	16.5	3.1	653
REG	DD	5.0	9.6	4.7	432
PUM	DD	14.9	12.0	12.7	377
REG	TD	26.2	32.0	5.7	406
PUM	TD	32.2	35.7	12.5	404
REG	PAR	52.4	60.2	11.9	428
ABL	PAR	53.2	60.6	18.9	421
PUM	PAR	52.9	60.8	22.7	407
OPC	PAR	51.7	60.4	7.6	407

*This is the age of the specimen after impregnation with PCM. ABL, autoclaved blocks; REG, regular concrete block; PUM, pumice concrete block; EXS, expanded shale (aggregate) block; OPC, ordinary Portland cement concrete; BS, butyl stearate; DD, dodecanol; TD, tetradecanol; PAR, paraffin [29].



Fig. 47. Photo of experimental house, Spain [40].

To extend the service life of bridge decks, by reducing the freeze/thaw damage, Sakulich and Bentz [141] incorporated PCM in cementitious mortar via fine lightweight aggregates. Two lightweight aggregates (expanded clay and pumice) and four PCM (a paraffin wax, vegetable oil based PCM, PEG400 and PEG600) were investigated. Test results showed that the compressive strength was lower in all PCM incorporated cement mortar with polyethylene glycol cement mortar showing a substantial reduction in compressive strength. The decrease in compressive strength was due to the mechanical (the relative weakness of LWA) and chemical reasons (polyethylene glycol interfering in hydration). Moreover, paraffin showed no effect on hydration reaction while polyethylene and vegetable oil-based PCM significantly retarded and suppressed the hydration of the cement mortar. This suggests that the PCM sticking to the aggregate surface were likely to be a problem during cement hydration. With the help of service life model developed by the authors, the locations in the United States where PCM incorporation can reduce freeze/thaw damage were proposed. In 104 out of 237 locations investigated, it was found that a conservative dosage of 50 kg/m^3 of PCM would increase the service life of bridge deck by at least 1 year. It is noteworthy to mention here that the focus of this section is on building application for phase change materials however, due to important contribution of this research it was discussed here. Moreover, the findings could be positively used for building applications.

Hunger et al. [142] experimental investigated the incorporation of different percentages of microencapsulated PCM (1, 3, 5%) on the material properties of self compacting concrete. Based on fresh properties test (J-ring and V-funnel test), all the mixes showed good self-compacting concrete properties. From heat of hydration results, the temperature peak of hydration could be reduced up to 28.1% by incorporating 5% PCM. However, heating rate could not be changed by the incorporation of microencapsulated PCM. It was shown that increasing the PCM content resulted in lower thermal conductivity and increased heat capacity, both of which significantly improved the thermal performance of concrete and resulted in energy saving of 12% (with 5% PCM). Moreover, the reduction in compressive strength of up to 69% was obtained with inclusion of 5% PCM. The reduction in compressive strength was due to (a) significant disparity between the intrinsic strength of the microcapsules and the concrete constituents and (b) damage of microcapsules during mixing resulting in leakage of paraffin and subsequent interference with the surrounding matrix. Even though the loss of compressive strength was significant, the compressive strength with 3% PCM was 35 N/mm^2, which is acceptable for most constructional purposes. Therefore, in order to enhance the compressive strength of concrete, it is suggested to incorporate microcapsules having stronger shell.

Castellon et al. investigated the thermal behavior of cubicles having dimensions of 2 m × 2 m × 3 m (Fig. 47) during 2005 and 2006 in Spain [40,143]. The panels (south, west and roof walls) were microencapsulated with 5 wt% PCM having melting point of 26 °C and latent heat of fusion 100 KJ/kg. The results observed during both summers were very good since temperature differences up to 4 °C were observed between reference cubicle and PCM-concrete cubicle. The maximum temperature in the walls with PCM appeared about 2 h later than non-PCM cubicle. Moreover, in order to have a real simulation of a building, the following sequences of experiments were performed.

Case 1. (Free cooling): The windows were opened at night and closed during the day.

Case 2. The windows located in the South wall were opened for the whole day.

Case 3. The windows were closed for the whole day.

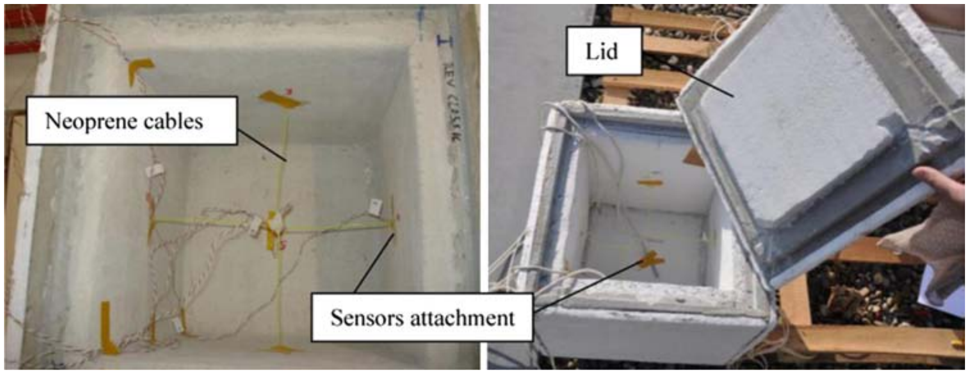


Fig. 48. Photo of test cells showing sensor arrangement [145].

Different results were obtained in every experiment, however according to the authors; the best option was the free cooling as it allowed the PCM to go through melting/solidification cycle. It is worth mentioning here that the microencapsulated PCM concrete reached a compressive strength of over 25 MPa and tensile splitting strength over 6 MPa (after 28 days). This opens a new venture for application of PCM-concrete for structural purposes.

The effect of microencapsulated PCM in concrete floors to store solar energy for moderate sea climate was investigated by Entrop et al. [144]. Four boxes (1130 mm × 725 mm × 690 mm) with two having 5 wt% PCM (Micronal DS 5008 X) in concrete floors were tested. It was found that the incorporation of microencapsulated PCM in concrete floors reduced the maximum floor temperature by up to 16 ± 2% and increased the minimum temperature by up to 7 ± 3%. Thus, PCM utilized in concrete can effectively store thermal energy without applying mechanical systems.

With the purpose of the enhancing the thermal comfort inside buildings, Sa et al. [145] incorporated 25% of microencapsulated paraffin powder into plastering mortar. Two cells (with and without PCM mortar) having an internal hollow volume of $26 \times 26 \times 26$ cm^3 were tested in climate chamber having dimensions of 58×76.5 and 75 cm^3 (Fig. 48). The thermal cycles in the climate chamber resembled scenarios for summer and spring in Portugal. Test results showed that the difference in the maximum internal temperature between the reference and PCM mortar cell was 2.6 °C for the spring day while this difference was 2 °C for the summer day. The numerical modeling of the experiment was also performed and the results were quite satisfactory.

An experimental investigation was carried out by Park et al. [146] to verify the applicability and fungal resistance of mortar and concrete containing zeolite and zeocarbon microcapsules (Figs. 49 and 50). D-Limonene was selected as the core material while zeolite and zeocarbon were added to prevent the damage of anti-fungal microcapsules membrane especially occurring during mixing and placing of mortar and concrete. Test results confirmed that zeolite and zeocarbon are effective in reducing the damage of microcapsules in mortar and concrete. From the fungal resistance test of mortar panel it was found that fungus did not grow on the surface of mortar panel containing antifungal microcapsules. Moreover, the addition of anti-fungal microcapsules increased slump and air content and decreased the compressive strength of mortar and concrete. The increase in slump was due to the ball bearing effect caused by the microcapsules during mixing while the compressive strength reduction was due to the significant disparity between the intrinsic strength of the microcapsules and the concrete constituents. However, the overall performance of the mortar and concrete (with and without antifungal microcapsules) was found to be similar. Furthermore, it was suggested to find the most effective mixing ratio of the anti-fungal microcapsules into mortar and concrete.

11. Conclusions and recommendations

Based on the analysis of published literature, following conclusions can be drawn.

- The properties of PCM would have direct impact on the human comfort. Therefore, the choice of a PCM for a given thermal energy storage application in buildings require careful examination of the thermo-physical, kinetic, chemical, economic and environmental properties of the various available candidates, comparing their merits and demerits and in some cases achieving a certain degree of compromise. Moreover, in order to be used in building envelope, target PCM materials shall have phase change temperatures in the human comfort zone.
- The use of microencapsulated PCM in construction materials is growing. However, in most of the research works, the performance of microencapsulated PCM has not been extensively compared with that of pure PCM. Therefore, it is suggested that researchers should undertake more comparative research works between pure PCM and microencapsulated PCM so as to evaluate the performance enrichment due to microencapsulation of PCMs. Researchers should focus on improving the strength of the microcapsules so as to reduce the significant disparity between the intrinsic strength of the microcapsules and the construction materials. Moreover, materials which are economical and available in abundance should be utilized for the development of microcapsules so as to reach commercial state.
- Shape stabilized PCM is a promising technique and should be studied future with more focus on its application especially in buildings.
- Various materials such as diatomite, expanded perlite and graphite, and vermiculite have been used as a container for the development of form-stable composite PCM. It has been shown that these materials are available in abundance. However, for successful utilization in building applications especially in cement based materials it needs to be ensured that these materials should not interfere with the hydration process and hydration products, affect the mechanical properties and durability of the building materials. Moreover, most of the researchers have focused on the development of form-stable composite PCM. Therefore, it is suggested that in future, researchers should also focus on applied investigation of form-stable composite PCM.
- The thermal properties provided by the manufacturers could be incorrect, doubtful and over optimized. Therefore, it is necessary to make measurements so as to get correct phase change properties of PCM.
- FT-IR, DSC, TGA and hot wire method have been widely used to determine the chemical compatibility, thermal properties,



Fig. 49. Optical microcope image of zeolite microcapsules [146].



Fig. 50. Optical microcope image of zeocarbon microcapsules [146].

thermal stability and thermal conductivity of composite PCM. It is necessary that these equipment should be calibrated so as to minimize any measurement uncertainty by ensuring accuracy of the equipment.

- Researchers and manufacturers have over the years used different approaches to obtain the properties of PCMs resulting in a wide variation in the data available on the properties of PCMs. Thus, there is a need to develop international standards to test thermal energy storage products.
- Wallboards and concrete are widely used in building applications and have a larger heat exchange area. This makes them appropriate for application of PCMs. The PCM enhanced wallboards and concrete are capable of reducing energy cost, scale of air-conditioning, the peak indoor air temperature and the fluctuation of indoor temperature. They can be very effective in transferring the heating and cooling loads away from the peak demand times. Moreover, they can contribute to reducing CO_2 emissions associated with heating and cooling. Nevertheless, for their generalized use, a lot of research needs to be focused on the durability, fire resistance and long term thermal behavior of PCM enhanced wallboards and concrete.

The literature on economic and environmental assessment of application of PCM in buildings is scarce. Therefore, more research should be focused on this area.

References

[1] Agency IE. Key world energy statistics. France: International Energy Agency; 2012; 80.
[2] Petroleum B. Statistical Review of World Energy. 2010.
[3] Administration USEI. How much energy is consumed in the world by each sector? United States of America 2013.
[4] Energy USDO. Buildings energy data book. United States of America: Energy efficiency & Renewable Energy; 2011.
[5] Pérez-Lombard L, Ortiz J, Pout C. A review on buildings energy consumption information. Energy Build 2008;40:394–8.
[6] Pasupathy A, Velraj R, Seeniraj RV. Phase change material-based building architecture for thermal management in residential and commercial establishments. Renew Sustain Energy Rev 2008;12:39–64.
[7] Sharma A, Tyagi VV, Chen CR, Buddhi D. Review on thermal energy storage with phase change materials and applications. Renew Sustain Energy Rev 2009;13:318–45.
[8] Regin AF, Solanki SC, Saini JS. Heat transfer characteristics of thermal energy storage system using PCM capsules: a review. Renew Sustain Energy Rev 2008;12:2438–58.
[9] Waqas A, Ud Din Z. Phase change material (PCM) storage for free cooling of buildings—a review. Renew Sustain Energy Rev 2013;18:607–25.
[10] Soares N, Costa JJ, Gaspar AR, Santos P. Review of passive PCM latent heat thermal energy storage systems towards buildings′ energy efficiency. Energy Build 2013;59:82–103.
[11] Zhou D, Zhao CY, Tian Y. Review on thermal energy storage with phase change materials (PCMs) in building applications. Appl Energy 2012; 92:593–605.
[12] Baetens R, Jelle BP, Gustavsen A. Phase change materials for building applications: a state-of-the-art review. Energy Build 2010;42:1361–8.
[13] Dincer I, Rosen MA. Thermal energy storage systems and applications. England: John Wiley and Sons; 2002.
[14] Abhat A. Low temperature latent heat thermal energy storage: heat storage materials. Sol Energy 1983;30:313–32.
[15] Kenisarin M, Mahkamov K. Solar energy storage using phase change materials. Renew Sustain Energy Rev 2007;11:1913–65.
[16] Kuznik F, David D, Johannes K, Roux J-J. A review on phase change materials integrated in building walls. Renew Sustain Energy Rev 2011;15:379–91.
[17] Cabeza LF, Castell A, Barreneche C. de Gracia A, Fernández AI. Materials used as PCM in thermal energy storage in buildings: a review. Renew Sustain Energy Rev 2011;15:1675–95.
[18] Zalba B, Marín JM, Cabeza LF, Mehling H. Review on thermal energy storage with phase change: materials, heat transfer analysis and applications. Appl Therm Eng 2003;23:251–83.
[19] Oró E, de Gracia A, Castell A, Farid MM, Cabeza LF. Review on phase change materials (PCMs) for cold thermal energy storage applications. Appl Energy 2012;99:513–33.
[20] Shen H, Tan H, Tzempelikos A. The effect of reflective coatings on building surface temperatures, indoor environment and energy consumption—an experimental study. Energy Build 2011;43:573–80.
[21] Mehling H, Cabeza LF. Heat and cold storage with PCM: an up to date introduction into basics and applications. Germany: Springer; 2008.
[22] Khudhair AM, Farid MM. A review on energy conservation in building applications with thermal storage by latent heat using phase change materials. Energy Convers Manage 2004;45:263–75.
[23] Bo H, Gustafsson EM, Setterwall F. Tetradecane and hexadecane binary mixtures as phase change materials (PCMs) for cool storage in district cooling systems. Energy 1999;24:1015–28.
[24] Tyagi VV, Buddhi D. PCM thermal storage in buildings: a state of art. Renew Sustain Energy Rev 2007;11:1146–66.
[25] Zhang Yinping, Yi J, Yi J. A simple method, the -history method, of determining the heat of fusion, specific heat and thermal conductivity of phase-change materials. Meas Sci Technol 1999:10.
[26] Kauranen P, Peippo K, Lund PD. An organic PCM storage system with adjustable melting temperature. Sol Energy 1991;46:275–8.
[27] Peippo K, Kauranen P, Lund PD. A multicomponent PCM wall optimized for passive solar heating. Energy Build 1991;17:259–70.
[28] Dimaano MNR, Watanabe T. Performance investigation of the capric and lauric acid mixture as latent heat energy storage for a cooling system. Sol Energy 2002;72:205–15.
[29] Hawes DW, Feldman D, Banu D. Latent heat storage in building materials. Energy Build 1993;20:77–86.
[30] Wada T, Yokotani F, Matsuo Y. Equilibria in the aqueous ternary system containing Na^{+}, CH_3CO^{-2}, and $P_2O_7^{4-}$ between 38 and 85°C. Bull Chem Soc Japan 1984;57:1672–3.
[31] Naumann R, Emons HH. Results of thermal analysis for investigation of salt hydrates as latent heat-storage materials. J Therm Anal 1989;35:1009–31.
[32] Hawes DW, Banu D, Feldman D. Latent heat storage in concrete. Sol Energy Mater 1989;19:335–48.
[33] Feldman D, Banu D, Hawes D, Ghanbari E. Obtaining an energy storing building material by direct incorporation of an organic phase change material in gypsum wallboard. Sol Energy Mater 1991;22:231–42.
[34] Hawlader MNA, Uddin MS, Khin MM, Microencapsulated PCM. thermal-energy storage system. Appl Energy 2003;74:195–202.
[35] Tyagi VV, Kaushik SC, Tyagi SK, Akiyama T. Development of phase change materials based microencapsulated technology for buildings: a review. Renew Sustain Energy Rev 2011;15:1373–91.
[36] Jegadheeswaran S, Pohekar SD. Performance enhancement in latent heat thermal storage system: a review. Renew Sustain Energy Rev 2009;13:2225–44.
[37] Alkan C, Sarı A, Karaipekli A, Uzun O. Preparation, characterization, and thermal properties of microencapsulated phase change material for thermal energy storage. Sol Energy Mater Sol Cells 2009;93:143–7.

[38] Özonur Y, Mazman M, Paksoy HÖ, Evliya H. Microencapsulation of coco fatty acid mixture for thermal energy storage with phase change material. Int J Energy Res 2006;30:741–9.
[39] Hawlader MNA, Uddin MS, Zhu HJ. Encapsulated phase change materials for thermal energy storage: experiments and simulation. Int J Energy Res 2002;26:159–71.
[40] Cabeza LF, Castellón C, Nogués M, Medrano M, Leppers R, Zubillaga O. Use of microencapsulated PCM in concrete walls for energy savings. Energy Build 2007;39:113–9.
[41] Lee SH, Yoon SJ, Kim YG, Choi YC, Kim JH, Lee JG. Development of building materials by using micro-encapsulated phase change material. Korean J Chem Eng 2007;24:332–5.
[42] Schossig P, Henning HM, Gschwander S, Haussmann T. Micro-encapsulated phase-change materials integrated into construction materials. Sol Energy Mater Sol Cells 2005;89:297–306.
[43] Raj VAA, Velraj R. Review on free cooling of buildings using phase change materials. Renew Sustain Energy Rev 2010;14:2819–29.
[44] Zhang YP, Lin KP, Yang R, Di HF, Jiang Y. Preparation, thermal performance and application of shape-stabilized PCM in energy efficient buildings. Energy Build 2006;38:1262–9.
[45] Sarı A. Form-stable paraffin/high density polyethylene composites as solid–liquid phase change material for thermal energy storage: preparation and thermal properties. Energy Convers Manage 2004;45:2033–42.
[46] Zhang Y, Ding J, Wang X, Yang R, Lin K. Influence of additives on thermal conductivity of shape-stabilized phase change material. Sol Energy Mater Sol Cells 2006;90:1692–702.
[47] Inaba H, Tu P. Evaluation of thermophysical characteristics on shape-stabilized paraffin as a solid-liquid phase change material. Heat Mass Transf 1997;32:307–12.
[48] Hong Y, Xin-shi G. Preparation of polyethylene–paraffin compound as a form-stable solid-liquid phase change material. Sol Energy Mater Sol Cells 2000;64:37–44.
[49] Xiao M, Feng B, Gong K. Thermal performance of a high conductive shape-stabilized thermal storage material. Sol Energy Mater Sol Cells 2001; 69:293–6.
[50] Cheng W-l Zhang R-m, Xie K, Liu N, Wang J. Heat conduction enhanced shape-stabilized paraffin/HDPE composite PCMs by graphite addition: preparation and thermal properties. Sol Energy Mater Sol Cells 2010;94:1636–1642.
[51] Karaipekli A, Sari A. Capric acid and palmitic acid eutectic mixture applied in building wallboard for latent heat thermal energy storage. J Sci Ind Res 2007;66:7.
[52] Sarı A, Karaipekli A. Preparation, thermal properties and thermal reliability of capric acid/expanded perlite composite for thermal energy storage. Mater Chem Phys 2008;109:459–64.
[53] Karaipekli A, Sarı A. Capric–myristic acid/vermiculite composite as form-stable phase change material for thermal energy storage. Sol Energy 2009;83:323–32.
[54] Zhang D, Zhou J, Wu K, Li Z. Granular phase changing composites for thermal energy storage. Sol Energy 2005;78:471–80.
[55] Memon SA, Lo TY, Cui H, Barbhuiya S. Preparation, characterization and thermal properties of dodecanol/cement as novel form-stable composite phase change material. Energy Build 2013;66:697–705.
[56] Karaman S, Karaipekli A, Sarı A, Biçer A. Polyethylene glycol (PEG)/diatomite composite as a novel form-stable phase change material for thermal energy storage. Sol Energy Mater Sol Cells 2011;95:1647–53.
[57] Sarı A, Karaipekli A. Fatty acid esters-based composite phase change materials for thermal energy storage in buildings. Appl Therm Eng 2012;37:208–16.
[58] Xu B, Li Z. Paraffin/diatomite composite phase change material incorporated cement-based composite for thermal energy storage. Appl Energy 2013;105:229–37.
[59] Li M, Kao H, Wu Z, Tan J. Study on preparation and thermal property of binary fatty acid and the binary fatty acids/diatomite composite phase change materials. Appl Energy 2011;88:1606–12.
[60] Brown TJ, Shaw RA, Bide T, Petavratzi E, Raycraft ER, Walters AS. World mineral production 2007–2011. Keyworth, Nottingham: British Geological Survey; 2013.
[61] Alkan M, Doğan M. Adsorption of Copper(II) onto Perlite. J Colloid Interfacial Sci 2001;243:280–91.
[62] Tekin N, Kadıncı E, Demirbaş Ö, Alkan M, Kara A, Doğan M. Surface properties of poly(vinylimidazole)-adsorbed expanded perlite. Microporous Mesoporous Mater 2006;93:125–33.
[63] Sarı A, Karaipekli A, Alkan C. Preparation, characterization and thermal properties of lauric acid/expanded perlite as novel form-stable composite phase change material. Chem Eng J 2009;155:899–904.
[64] Sarı A, Karaipekli A. Preparation, thermal properties and thermal reliability of palmitic acid/expanded graphite composite as form-stable PCM for thermal energy storage. Sol Energy Mater Sol Cells 2009;93:571–6.
[65] Zhang Z, Shi G, Wang S, Fang X, Liu X. Thermal energy storage cement mortar containing n-octadecane/expanded graphite composite phase change material. Renew Energy 2013;50:670–5.
[66] Wang W, Yang X, Fang Y, Ding J, Yan J. Preparation and thermal properties of polyethylene glycol/expanded graphite blends for energy storage. Appl Energy 2009;86:1479–83.
[67] Wang Y, Xia TD, Zheng H, Feng HX. Stearic acid/silica fume composite as form-stable phase change material for thermal energy storage. Energy Build 2011;43:2365–70.
[68] Mehta PK, Monteiro PJM. Concrete: microstructure, properties and materials. USA: McGraw-Hill; 2006.
[69] Hall MR. Hygrothermal materials for heat and moisture control in buildings. In: Hall M R, editor. Materials for energy efficiency and thermal comfort in buildings. United Kingkom: Woodhead publishing limited; 2010.
[70] Wilson IR. Kaolin and halloysite deposits of China. Clay Miner 2004;39:1–15.
[71] Panda AK, Mishra BG, Mishra DK, Singh RK. Effect of sulphuric acid treatment on the physico-chemical characteristics of kaolin clay. Colloid Surf A: Physicochem Eng Asp 2010;363:98–104.
[72] Madejová J. FTIR techniques in clay mineral studies. Vibr Spectrosc 2003;31:1–10.
[73] Belver C, Mun~ oz MABa, Vicente MA. Chemical activation of a Kaolinite under acid and alkaline conditions. Chem Mater 2002;14:11.
[74] Vu DD, Stroeven P, Bui VB. Strength and durability aspects of calcined kaolin-blended Portland cement mortar and concrete. Cem Conc Compos 2001;23:471–8.
[75] Ali Memon S, Yiu Lo T, Shi X, Barbhuiya S, Cui H. Preparation, characterization and thermal properties of Lauryl alcohol/Kaolin as novel form-stable composite phase change material for thermal energy storage in buildings. Appl Therm Eng 2013;59:336–47.
[76] Siddique R. Waste materials and by-products in concrete. Berlin: Springer; 2008.
[77] Puertas F, Martínez-Ramírez S, Alonso S, Vázquez T. Alkali-activated fly ash/slag cements: strength behaviour and hydration products. Cement Conc Res 2000;30:1625–32.
[78] Aßbrock O, Brameshuber W, Droll K, Lang E, Motz H, Müller C, et al. Ground Granulated Blast Furnace Slag (GGBS) as a concrete additive. Germany: The Federal Association of the German Ready-Mixed Concrete Industry, FEhS – Institute for Building Materials- Research, Association of German Cement Works; 2007. p. 135.
[79] Memon SA, Lo TY, Barbhuiya SA, Xu W. Development of form-stable composite phase change material by incorporation of dodecyl alcohol into ground granulated blast furnace slag. Energy Build 2013;62:360–7.
[80] Topçu İB, Canbaz M. Properties of concrete containing waste glass. Cement and Concrete Research 2004;34:267–74.
[81] Environmental protection department TGotHK, SAR. Hong Kong′s Environment, Glass container recycling programme. Hong Kong 2012.
[82] Ling T-C, Poon C-S, Kou S-C. Feasibility of using recycled glass in architectural cement mortars. Cem Conc Compos 2011;33:848–54.
[83] Memon SA, Lo TY, Cui H. Utilization of waste glass powder for latent heat storage application in buildings. Energy Build 2013;66:405–14.
[84] Chen Z, Shan F, Cao L, Fang G. Preparation and thermal properties of n-octadecane/molecular sieve composites as form-stable thermal energy storage materials for buildings. Energy Build 2012;49:423–8.
[85] Li M, Wu Z, Kao H. Study on preparation, structure and thermal energy storage property of capric–palmitic acid/attapulgite composite phase change materials. Appl Energy 2011;88:3125–32.
[86] Karaipekli A, Sarı A. Preparation and characterization of fatty acid ester/building material composites for thermal energy storage in buildings. Energy Build 2011;43:1952–9.
[87] Watson ES, Ridgefield, O′Neill MJ. Differential microcalorimeter. In: Office USP, editor. United States 1966.
[88] Wunderlich B. Thermal analysis. United States of America: New York Academic; 1990.
[89] Haines PJ, Reading M, Wilburn FW. Differential thermal analysis and differential scanning calorimetry. In: Brown ME, editor. Handbook of thermal analysis and calorimetry. The Netherlands: Elsevier; 1998.
[90] Instruments T. DSC 2010 Differential scanning calorimeter operator′s manual. United Kingdom1998.
[91] Instruments T. Differential scanning calorimetry. 2013.
[92] Instruments T. DSC. 2012.
[93] Instrumentation T. What is calibration and why is it so important? United Kingdom: Tempcon Instrumentation; 2013.
[94] Marangoni AG, Wesdorp LH. Structure and properties of fat crystal network. United States of America: CRC Press Taylor and Fransis Group; 2012.
[95] Gill P, Moghadam TT, Ranjbar B. Differential scanning calorimetry techniques: applications in biology and nanoscience. J Biomol Tech 2010;21:27.
[96] Danley RL. New heat flux DSC measurement technique. Thermochim Acta 2002;395:8.
[97] Instruments T. TA Instruments Universal Analysis 2000. 4.5 A ed1998.
[98] Murphy CB. Review of fundamental developments in analysis differential thermal analysis. Anal Chem 1958;30:6.
[99] Marín JM, Zalba B, Cabeza LF, Mehling H. Determination of enthalpy–temperature curves of phase change materials with the temperature-history method: improvement to temperature dependent properties. Meas Sci Technol 2003;14:184.
[100] Peck JH, Kim J-J, Kang C, Hong H. A study of accurate latent heat measurement for a PCM with a low melting temperature using T-history method. Int J Refrig 2006;29:1225–32.
[101] Hong H, Kim SK, Kim Y-S. Accuracy improvement of T-history method for measuring heat of fusion of various materials. Int J Refrig 2004;27:360–6.

[102] Barth A, Parvez H. Advances in biomedical spectroscopy. In: Barth A, Haris PI, editors. Bilogical and biomedical infrared spectroscopy. Netherlands: IOS Press BV; 2009.
[103] Coates J. Intrepretation of Infrared spectra, a practical approach. In: Meyers RA, editor. Encyclopedia of analytical chemistry. John Wiley & Sons Ltd; 2000.
[104] Corporation TN. Introduction to fourier transform infrared spectrometry. 2001.
[105] Wikipedia. Fourier transform infrared spectroscopy. Wikipedia; 2013.
[106] Specac. Manual hydraulic press - 15 and 25 t. United Kingdom: Specac; 2013.
[107] Volland W. Organic compound identification using infrared spectroscopy. Washington 1999.
[108] Coats AW, Redfern JP. Thermogravimetric analysis a review. Analyst 1963:88.
[109] Elmer P. Thermogravimetric analysis (TGA) a beginner's guide. United States of America: Perkin Elmer; 2010.
[110] Elmer P. Installation help manual. United States of America: Perkin Elmer; 2007.
[111] Elmer P. STA 6000 Simultaneous thermal analyzer. United States of America: Perkin Elmer; 2008.
[112] Wikipedia. Thermal conductivity measurement. Wikipedia; 2013.
[113] ASTM. Standard Test Method for Steady State Thermal Transmission Properties by Means of the Heat Flow Meter Apparatus. United States of America: ASTM International; 2010. p. 15.
[114] GmbH N-G. Heat flow meter HFM 436/3 LambdaTM. In: GmbH N-G, editor. Bavaria 2008. p. 84.
[115] ASTM. Standard test method for thermal conductivity of solids by means of the guarded-comparative-longitudinal heat flow technique. United States of America: ASTM International; 2010.
[116] Instruments T. Principal methods of thermal conductivity measurement. 2012.
[117] Karaipekli A, Sarı A, Kaygusuz K. Thermal conductivity improvement of stearic acid using expanded graphite and carbon fiber for energy storage applications. Renew Energy 2007;32:2201–10.
[118] Frusteri F, Leonardi V, Vasta S, Restuccia G. Thermal conductivity measurement of a PCM based storage system containing carbon fibers. Appl Therm Eng 2005;25:1623–33.
[119] ASTM. Standard Test Method for thermal conductivity of refractories by hot wire (Platinum Resistance Thermometer Technique). United States of America: ASTM International; 2009. p. 6.
[120] Velraj R, Seeniraj RV, Hafner B, Faber C, Schwarzer K. Heat transfer enhancement in a latent heat storage system. Sol Energy 1999;65:171–80.
[121] Farid MM, Khudhair AM, Razack SAK, Al-Hallaj S. A review on phase change energy storage: materials and applications. Energy Convers Manage 2004;45:1597–615.
[122] Agyenim F, Hewitt N, Eames P, Smyth M. A review of materials, heat transfer and phase change problem formulation for latent heat thermal energy storage systems (LHTESS). Renew Sustain Energy Rev 2010;14:615–28.
[123] Scalat S, Banu D, Hawes D, Parish J, Haghighata F, Feldman D. Full scale thermal testing of latent heat storage in wallboard. Sol Energy Mater Sol Cells 1996;44:49–61.
[124] Shilei L, Neng Z, Guohui F. Impact of phase change wall room on indoor thermal environment in winter. Energy Build 2006;38:18–24.
[125] Kuznik F, Virgone J. Experimental assessment of a phase change material for wall building use. Appl Energy 2009;86:2038–46.
[126] Kuznik F, Virgone J, Johannes K. In-situ study of thermal comfort enhancement in a renovated building equipped with phase change material wallboard. Renew Energy 2011;36:1458–62.
[127] Kuznik F, Virgone J. Experimental investigation of wallboard containing phase change material: data for validation of numerical modeling. Energy Build 2009;41:561–70.
[128] Neeper DA. Thermal dynamics of wallboard with latent heat storage. Sol Energy 2000;68:393–403.
[129] Athienitis AK, Liu C, Hawes D, Banu D, Feldman D. Investigation of the thermal performance of a passive solar test-room with wall latent heat storage. Build Environ 1997;32:405–10.
[130] Oliver A. Thermal characterization of gypsum boards with PCM included: thermal energy storage in buildings through latent heat. Energy Build 2012;48:1–7.
[131] Ahmad M, Bontemps A, Sallée H, Quenard D. Experimental investigation and computer simulation of thermal behaviour of wallboards containing a phase change material. Energy Build 2006;38:357–66.
[132] Ahmad M, Bontemps A, Sallée H, Quenard D. Thermal testing and numerical simulation of a prototype cell using light wallboards coupling vacuum isolation panels and phase change material. Energy Build 2006;38:673–81.
[133] Borreguero AM, Carmona M, Sanchez ML, Valverde JL, Rodriguez JF. Improvement of the thermal behaviour of gypsum blocks by the incorporation of microcapsules containing PCMS obtained by suspension polymerization with an optimal core/coating mass ratio. Appl Therm Eng 2010;30:1164–9.
[134] Sarı A, Karaipekli A, Kaygusuz K. Capric acid and stearic acid mixture impregnated with gypsum wallboard for low-temperature latent heat thermal energy storage. Int J Energy Res 2008;32:154–60.
[135] Chan ALS. Energy and environmental performance of building façades integrated with phase change material in subtropical Hong Kong. Energy Build 2011;43:2947–55.
[136] Bentz DP, Turpin R. Potential applications of phase change materials in concrete technology. Cem Conc Compos 2007;29:527–32.
[137] Hawes DW, Banu D, Feldman D. Latent heat storage in concrete. II. Sol Energy Mater 1990;21:61–80.
[138] Lee T, Hawes DW, Banu D, Feldman D. Control aspects of latent heat storage and recovery in concrete. Sol Energy Mater Sol Cells 2000;62:217–37.
[139] Hadjieva M, Stoykov R, Filipova T. Composite salt-hydrate concrete system for building energy storage. Renew Energy 2000;19:111–5.
[140] Zhang D, Li Z, Zhou J, Wu K. Development of thermal energy storage concrete. Cement Conc Res 2004;34:927–34.
[141] Sakulich AR, Bentz DP. Incorporation of phase change materials in cementitious systems via fine lightweight aggregate. Constr Build Mater 2012;35:483–90.
[142] Hunger M, Entrop AG, Mandilaras I, Brouwers HJH, Founti M. The behavior of self-compacting concrete containing micro-encapsulated Phase Change Materials. Cem Conc Compos 2009;31:731–43.
[143] Castellón C, Medrano M, Roca J, Nogués M, Castell A, Cabeza LF. Use of microencapsulated PCM in concrete walls for energy savings. ASHRAE 2007:6.
[144] Entrop AG, Brouwers HJH. Reinders AHME. Experimental research on the use of micro-encapsulated Phase Change Materials to store solar energy in concrete floors and to save energy in Dutch houses. Sol Energy 2011;85:1007–20.
[145] Sá AV, Azenha M, de Sousa H, Samagaio A. Thermal enhancement of plastering mortars with phase change materials: experimental and numerical approach. Energy Build 2012;49:16–27.
[146] Park S-K, Kim J-HJ, Nam J-W, Phan HD, Kim J-K. Development of anti-fungal mortar and concrete using Zeolite and Zeocarbon microcapsules. Cem Conc Compos 2009;31:447–53.